의학박사 학위논문

Encoding strategies of primary somatosensory cortex for touch and pain in physiological and pathological conditions

생리 및 병리적 조건에서 촉각과 통증에 대한
일차 체성감각 피질의 암호화 전략

2019 년 08 월

서울대학교 대학원
의과학과 생리학전공
김 유 림

Ph.D. Dissertation of Biomedical Sciences

생리 및 병리적 조건에서 촉각과 통증에 대한 일차 체성감각 피질의 암호화 전략

Encoding strategies of primary somatosensory cortex for touch and pain in physiological and pathological conditions

August 2019

Department of Biomedical Sciences
Seoul National University
College of Medicine
Yoo Rim Kim

생리 및 병리적 조건에서 촉각과 통증에 대한 일차 체성감각 피질의 암호화 전략

지도 교수 김 상 정

이 논문을 의학박사 학위논문으로 제출함

2019년 04월

서울대학교 대학원
의과학과 생리학전공

김 유 림

김유림의 의학박사 학위논문을 인준함
2019년 07월

위 원 장 _____(Seal)
부위원장 _____(Seal)
위 원 _____(Seal)
위 원 _____(Seal)
위 원 _____(Seal)

Encoding strategies of primary somatosensory cortex for touch and pain in physiological and pathological conditions

A Dissertation Submitted to the Faculty of the
Department of Biomedical Sciences
at
Seoul National University
by

Yoo Rim Kim

in Partial Fulfillment of the
Requirements for the Degree of
Doctor of Philosophy

Advisor: Sang Jeong Kim
April 2019

Approved by Thesis Committee:
July 2019

Chair _____ (Seal)
Vice Chair _____ (Seal)
Examiner _____ (Seal)
Examiner _____ (Seal)
Examiner _____ (Seal)

Abstract

Encoding strategies of primary somatosensory cortex for touch and pain in physiological and pathological conditions

Yoo Rim Kim
Department of Biomedical Sciences (Physiology major)
The Graduate School
Seoul National University College of Medicine

Primary somatosensory cortex (S1) plays an important role in the perception and discrimination of touch and pain. Conventionally, neurons in the somatosensory system including S1 cortex have been classified by noxiousness feature with innocuous brush and noxious pinch stimuli. Besides this noxiousness feature, each stimulus also includes other stimulus features, such as different textures or dynamics. However, it remains unexplored how S1 neurons comprehensively encode such diverse features of cutaneous stimuli at single-cell and population levels.

Tissue or nerve injury can lead to an inflammatory or neuropathic pain, in which hypersensitivity is accompanied. However, it is unclear how the response properties of S1 neurons towards mechanical stimuli are altered. It is also unknown how these S1 response changes are involved in pain hypersensitivity.

I investigated how S1 neurons comprehensively encode multiple stimulus features for touch and pain in physiological conditions and how the response properties of S1 neurons are changed in pain hypersensitivity. To explore this, using *in vivo* two-photon Ca^{2+} imaging, I recorded neural activities of S1 neurons in mice while

applying innocuous and noxious mechanical stimuli into hind paw.

This thesis is composed of two research parts on response properties of S1 neurons to touch and pain. In chapter 1, it is shown that S1 neurons exhibited highly selective response to the difference in texture (specificity coding), but low selectivity to the difference in dynamics or noxiousness with slightly more specificity to dynamics (pattern coding). In chapter 2, I found some of the noxious-preferred neurons, which responded to noxious pinch stimuli at normal states, responded to innocuous touch stimuli in CFA-induced hypersensitivity. The majority of broadly tuned neurons, however, maintained their normal tuning properties during hypersensitivity, but some of those showed increased responses to both innocuous and noxious mechanical stimuli in CFA-induced hypersensitivity.

This thesis demonstrates that S1 neurons use a mixed strategy of specificity coding and pattern coding for multiple stimulus features in a feature-dependent manner. In addition, it is also revealed how S1 cortex contributes to CFA-induced hypersensitivity in a way that tuning properties are changed and activities of broadly tuned neurons are generally increased in CFA-induced hypersensitivity. These findings would be important to understand the encoding rules and response properties of S1 to touch and pain in physiological and pathological conditions.

Keywords: touch, pain, primary somatosensory cortex, neural encoding, two-photon Ca^{2+} imaging, hypersensitivity
Student Number: 2010-23737

Table of Contents

Chapter 1

Differential selectivity of S1 neurons to multiple stimulus features of touch and pain

Introduction

It is well known that the primary somatosensory (S1) cortex plays an important role in the perception and discrimination of the mechanosensations. The S1 cortex receives innocuous and noxious somatosensory inputs from the thalamus, and is involved in sensory-discriminative aspects of pain including location, duration, and intensity (Bushnell et al., 1999; Apkarian et al., 2005; Basbaum et al., 2009). So far, electrophysiological studies investigating the role of S1 cortex for touch and pain have often focused on the responses of single neurons (Matsumoto et al., 1987; Quiton et al., 2010; Whitsel et al., 2010), or the population response for stimuli with a single feature (Reed et al., 2008; Lefort et al., 2009), limiting the opportunity of understanding the population-level encoding strategy of S1 cortex for multiple features. Hence, the unexplored question is how multiple S1 neurons simultaneously encode diverse features of touch and pain sensation, such as noxiousness, texture, or dynamics.

Traditionally, the somatosensory neurons in the central nervous system (CNS) have been classified as low threshold (LT), high threshold (HT) or wide dynamic range (WDR) neurons according to their electrophysiological responses to innocuous and noxious stimuli. For instance, neurons that respond best to brush-stroke are

classified as LT; neurons only responsive to pinching with forceps are classified as HT; those responding to both brush and pinch but more intensely to pinch stimulus are classified as WDR (Lamour et al., 1983; Chung et al., 1986; Senapati et al., 2005). Despite the widespread adoption of this approach to identify the characteristics of the neurons in terms of the noxiousness (innocuous/noxious) or intensity (weak/strong) feature, however, it should be recognized that those stimuli can be qualitatively different (Chung et al., 1986). They are not only characterized by features such as noxiousness and intensity, but also by texture (brush hairs/forceps steel arm) and dynamics (dynamic stroke/static press), even though simple interpretations such as LT or HT have been made in many previous studies. In particular, this consideration will be more important if the neurons of interest can process multiple features of information. S1 neurons seem to be able to encode diverse features of sensory information compared to neurons in the spinal cord (Carter et al., 2014; Saal and Bensmaia, 2014), where the concept of LT/HT/WDR was originally proposed.

There has been a long debate between two opposite ideas about how the sensory information of touch and pain are encoded in the peripheral and central nervous system (Perl, 2007; Moayedi and Davis, 2013; Prescott et al., 2014). “Specificity” theory suggests that

different stimuli with different features are processed along distinct neurons with highly specific sensitivities, so called “labeled lines”. In contrast, “pattern” theory argues that the information about the stimulus feature is processed by distributed patterns of neural populations with low specificity at the individual cell level. Currently, it is evident that there exist specialized sensory organs for innocuous and noxious stimuli at primary afferent level, while it still remains unclear how the information from the labeled lines generate touch and pain perception in the central nervous system.

Here, I used *in vivo* two-photon Ca^{2+} imaging to simultaneously record the activity of layer 2/3 neurons in the S1 cortex in lightly anesthetized mice in response to cutaneous stimuli using brush and forceps with diverse features such as noxiousness, intensity, texture, and dynamics. I identified individual neurons with distinct tuning properties to texture, dynamics and noxiousness features of the cutaneous stimuli, as well as many broadly tuned neurons. Overall, the majority of the tuned neurons showed highly selective response to the difference in texture, but low selectivity to the difference in dynamics or noxiousness. Both dynamics and noxiousness features could be decoded using the response patterns of neural populations, implying all the relevant information of these features is being processed in a distributed manner in the S1 cortex. These findings

suggest a mixed specificity and pattern encoding strategy for multiple stimulus features by S1 neurons, and also suggest that the tuning property of S1 neurons does not match with the previous concept of LT/HT/WDR. It would be important for understanding the encoding strategy of S1 for touch and pain.

Results

Neural response patterns to innocuous and noxious stimuli in the S1 cortex of mouse

For in vivo two-photon Ca^{2+} imaging, a cranial window was made over the left S1 cortex hind paw area. The animal skull was opened corresponding to the S1 cortex (**Figure 1A**) and I injected adeno-associated virus expressing GCaMP6s. Using brush or stainless forceps, different types of cutaneous stimuli were applied to the right hind paw while recording Ca^{2+} fluorescence of S1 neurons in lightly anesthetized mice expressing GCaMP6s. When we applied pinch stimulation to the hind paw of the animal, we found that some of the S1 neurons significantly responded to the pinch stimulation compared to resting state (**Figure 1B**). After that, I investigated how S1 neurons comprehensively encode innocuous and noxious cutaneous stimuli in the S1 neurons.

Using two-photon Ca^{2+} imaging in lightly anesthetized mice expressing GCaMP6s in the layer 2/3 neurons of the left S1 cortex, I first tried to determine the response of S1 neurons by applying innocuous brushing and noxious pinch stimuli to the right hind paw as conventionally done in pain studies. However, since these two stimuli with the different noxiousness feature also have distinct texture and

dynamics features, I added another innocuous stimulation, Press, in this first experiment session (**Figure 2A, B and Table 1**). My idea is that if the neural response patterns to Press are similar to those to Brush, but not to Pinch, it indicates a fine tuning of S1 neurons to the noxiousness feature; in the opposite case, it means that S1 neurons are highly tuned to the texture or dynamics feature.

To analyze neuronal response patterns to different stimuli, I calculated the preference index (PI) of individual cells to each stimuli based upon their response amplitude and fidelity (see Materials and Methods). About a half of the responding neurons (fluorescence change > 30 % of F_0) were tuned to all the three stimuli (50.2%) and the majority of the other preferentially responded to either of Brush (17.0%) or Press · Pinch (13.4%). Interestingly, Press-responsive neurons also exhibited Ca^{2+} responses to Pinch with higher amplitude, rather than to Brush (**Figure 2C, D**). PI scatter plots between two stimuli indicated that S1 neurons have low selectivity to Press versus Pinch, but high selectivity to Press (or Pinch) versus Brush (n = 217 cells from 4 mice, **Figure 2D**). PCA, which represents population activity patterns, also showed that Press and Pinch evoke distinct, but very close neural population responses each other, which were clearly separated from those of Brush (N = 4 mice, **Figure 2E, F**). Taken together, these results suggest that S1 neurons are more

finely tuned to the texture or dynamics feature compared to the noxiousness/intensity feature.

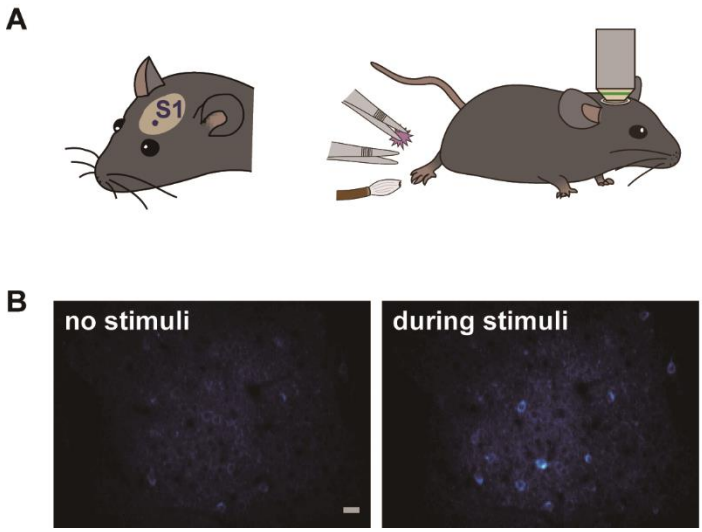

Figure 1 | Schematic diagrams of in vivo two-photon Ca^{2+} imaging in the mouse S1 cortex

(A) A craniotomy was made over the S1 cortex corresponding to the hind limb in the left hemisphere and three types of sensory stimuli were delivered to the right hind paw of anesthetized head-fixed mice using brush and forceps. **(B)** Representative in vivo two-photon Ca^{2+} fluorescence images of layer 2/3 S1 neurons during rest and pinch stimulation with forceps. Scale bar, 20 μm.

<table>
<tr><th>Figure 2</th><th>Figure 3</th><th colspan="2">Figure 5</th></tr>
<tr><td>Brush</td><td>B-stroke</td><td colspan="2"></td></tr>
<tr><td></td><td>B-press</td><td colspan="2"></td></tr>
<tr><td></td><td>F-stroke</td><td colspan="2"></td></tr>
<tr><td rowspan="2">Press</td><td rowspan="2">F-press</td><td colspan="2"></td></tr>
<tr><td></td><td>P0</td></tr>
<tr><td rowspan="3">Pinch</td><td rowspan="3"></td><td rowspan="3">F-pinch</td><td>P1</td></tr>
<tr><td>P2</td></tr>
<tr><td>P3</td></tr>
</table>

TABLE 1 | Explanatory table for the different types of stimuli applied to the experiment in each figure using brush or forceps

Innocuous Brush, Innocuous Press and noxious Pinch stimulus are applied in Figure 2. B-stroke and F-press are relabeled terms of Brush and Press stimulus in Figure 2, respectively, and in addition, B-press and F-stroke are added in Figure 3. The Pinch stimulus in Figure 2 is applied in four different intensities in Figure 5.

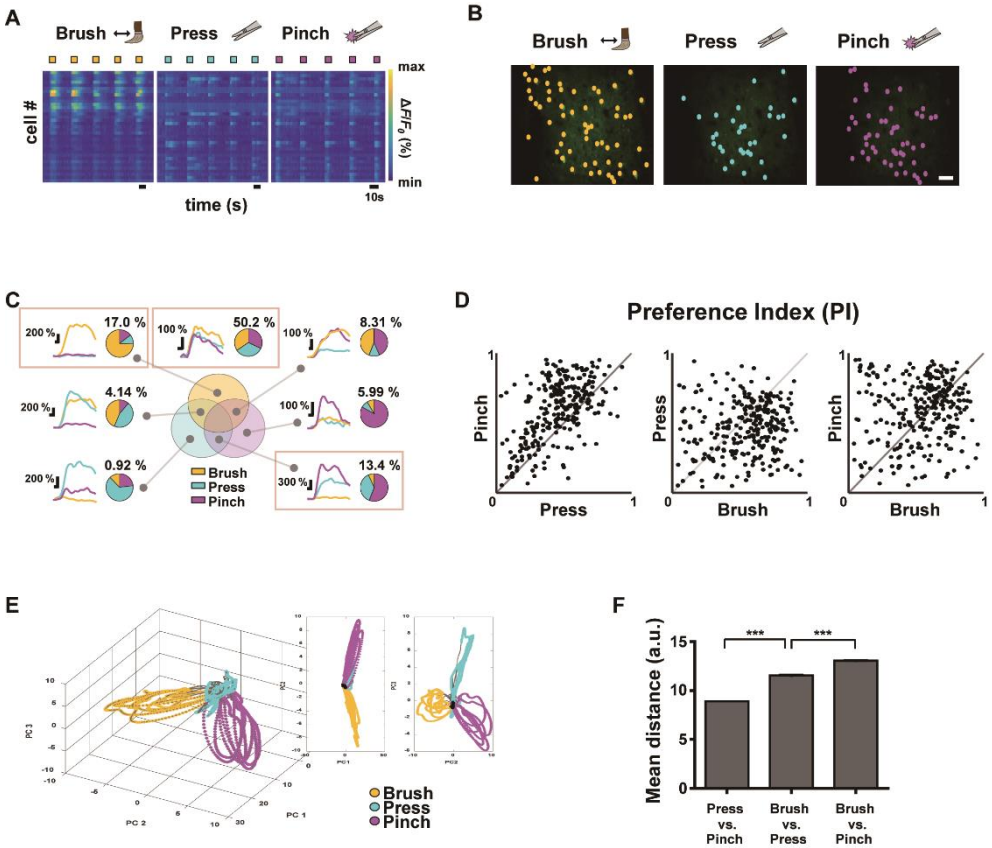

Figure 2 | Neural response properties evoked by innocuous and noxious stimuli in the mouse S1 cortex

(A) Color-coded raster plots of representative Ca^{2+} transients in S1 neurons in response to Brush, Press and Pinch. Each stimulus was applied five trials for 5s. Color-coded $\Delta F/F_0$ (%) ranges from 0 to 1000. Scale bar, 10s. **(B)** Spatial distribution of responsive neurons to Brush (yellow), Press (cyan) or Pinch (purple) for an example mouse. Scale bar, 50 μm. **(C)** Seven types of Ca^{2+} responses of the neurons responding to three different stimuli: On the right side of each response type, a representative pie chart shows proportions of the neurons responding to Brush (yellow), Press (cyan) and Pinch (purple), and their percentage to the total. Each portion of the Venn diagram corresponds to a type of neurons. Three red boxed figures point the proportions of Brush specific (17.0 %), Press/Pinch preferred (13.4 %) and broadly tuned (50.2 %) neurons (n = 217 cells from 4 mice).

(D) Scatter plots of the preference indexes (PIs) of individual neurons for two different stimuli: (Left) Press versus Pinch; (Middle) Brush versus Press; (Right) Brush versus Pinch (n = 217 cells from 4 mice). **(E)** An example of state-space representation of population activity patterns in response to the three stimuli from an example mouse. N-dimensional activity patterns (N, number of cells) over time were projected onto their two or three principal components via dimensionality reduction method. Each color (yellow, cyan, and purple) corresponds to each type of the stimuli. Black dots indicate states before stimuli onset and grey dots indicate states of inter-stimuli time. **(F)** Mean Euclidean distances between states in the state-space represented in (E). Distances were calculated between states in Press versus Pinch (8.92 ± 0.01, 46,872 pairs from four mice), Brush versus Press (11.54 ± 0.02, 47,524 pairs from four mice) and Brush versus Pinch (13.05 ± 0.03, 47,304 pairs from four mice). Data are represented as mean ± s.e.m. Statistics was performed with one-way ANOVA with Tukey's post-hoc test, F = 6577, ***p < 0.001.

Encoding texture and dynamics features of innocuous stimuli by S1 neurons

To comprehensively investigate how S1 neurons differentially encode the texture and the dynamics of mechanical stimuli, I recorded neuronal Ca^{2+} activity in the S1 cortex evoked by Brush−stroke (B−stroke), Brush−press (B−press), Forceps−stroke (F−stroke) and Forceps−press (F−press) hind paw stimuli (Figure 3A, Table 1 and Table 2). B−stroke and F−press are relabeled terms of Brush and Press stimulus in Figure 2, respectively, and in addition, B−press and F−stroke were added for more comprehensive investigation. From a variety of response patterns of individual neurons (Figure 3A, B), I found that B−stroke (F−stroke) responsive neurons also showed Ca^{2+} activities in response to B−press (F−press), rather than to F−stroke/press (B−stroke/press, respectively). The proportion of texture−discriminative neurons, preferentially responding to B−stroke and B−press (F−stroke and F−press) regardless of the dynamics feature, was much higher than that of dynamics−discriminative neurons, preferentially responding to B−stroke and F−stroke (B−press and F−press) stimulus regardless of the texture (n = 208 cells from 4 mice, Figure 3C). Hierarchical clustering analysis suggests that S1 neurons are primarily categorized by their Ca^{2+} responses to the different

textures, and secondarily by those to the different dynamics (Figure 3D). PI scatter plots also indicate that S1 neurons have relatively low selectivity to the dynamics (i.e. F−press versus F−stroke), but show high selectivity to the texture (i.e. F−press versus B−press) (n = 208 cells from 4 mice, Figure 3E). PCA also showed that neural population response patterns to four different stimuli can be separated, but B−stroke evokes similar response patterns to those by B−press, while relatively distinct from those by F−stroke/press (Figure 3F, G). There might be confounding features that could bias my interpretation of the selective response of S1 neurons in texture experiments, such as temperature or indentation depth of the stimuli. In other words, selective responses of S1 neurons for the different texture stimuli might be caused by the subtle difference in surface temperature or intensity of pressures between the brush and the forceps steel arm. To rule out this possibility, first, I measured the surface temperature of brush and forceps using an infrared thermometer (Figure 4A). The temperature difference between the two stimulation tools was only 0.5 ° C. This tiny difference does not cause selective responses of S1 neurons (Milenkovic et al., 2014). I then applied two pressures with different intensity (20g and 50g) to the hind paw in a random order, assuming that the difference in indentation depth induced by the two stimulation tools is not as large

as those by these two pressure stimuli (N = 3 mice, **Figure 4B–D**). PI scatter plots showed that the neurons have similar response patterns to the pressure stimuli with different indentation depth in terms of the fidelity and response amplitude. Calcium response amplitude of cells differed between the two pressures, but the proportion of the responding cells was not significantly different. Although there are several neurons with difference in response amplitudes between the pressures, it is difficult to say that the small difference in force has contributed to the selective response in S1 individual neurons (Ferrington et al., 1988; Moehring et al., 2018). Therefore, it is unlikely that subtle differences in temperature or indentation depth caused by the stimuli with the brush and forceps affect the observed selective responses in the texture experiments. Taken together, these results suggest that S1 neurons are more selective to the texture than dynamics at individual cell level.

			Texture	Noxiousness	Dynamics
Figure 3	B-stroke		Brush	Innocuous	Dynamic
	B-press			Innocuous	Static
	F-stroke		Forceps	Innocuous	Dynamic
	F-press			Innocuous	Static
Figure 5	F-pinch	P0	Forceps	Innocuous	Static
		P1		Noxious	
		P2			
		P3			

TABLE 2 | Explanatory table for the different types of stimuli applied to the experiment in Figure 3 and Figure 5

Each stimulus was classified by texture, noxiousness and dynamics using brush or forceps. F-pinch stimulus was subdivided into four intensities. P0<2g, P1=100g, P2=200g and P3=300g.

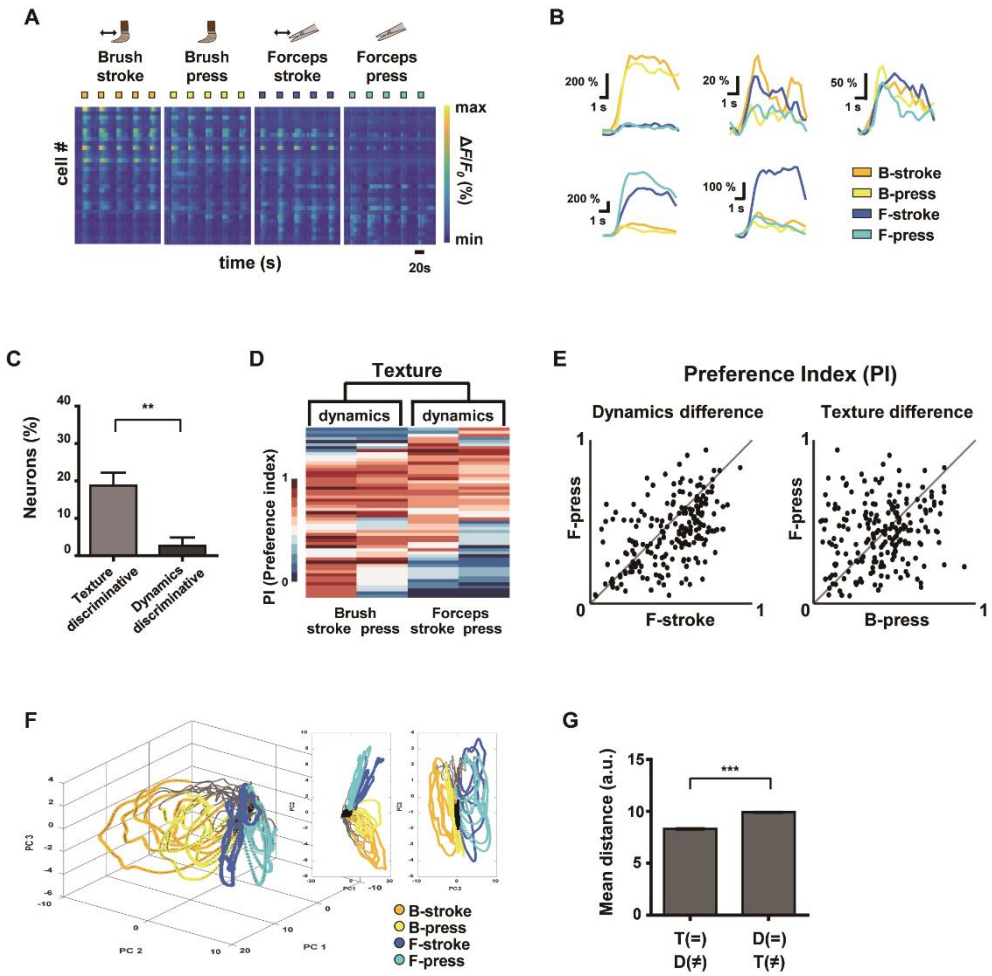

Figure 3 | Differential encoding of texture and dynamics features of innocuous stimuli by S1 neurons

(A) Color-coded raster plots of representative Ca^{2+} transients in S1 neurons in response to Brush-stroke, Brush-press, Forceps-stroke and Forceps-press. Each stimulus was applied five trials for 5s. Color-coded $\Delta F/F_0$ (%) ranges from 0 to 800. **(B)** Examples of various Ca^{2+} responses from five neurons to B-stroke (yellow), B-press (light-yellow), F-stroke (blue) and F-press (cyan) stimuli. **(C)** The percentage of texture-discriminative neurons (preferentially responsive to B-stroke/B-press or F-stroke/F-press, 18.75% ± 3.43%) and that of dynamics-discriminative (preferentially responsive to B-stroke/F-stroke or B-press/F-press, 2.67% ± 2.21%) neurons. Data are represented as mean ± s.e.m.

Statistics was performed with a two-tailed unpaired t-test (n = 208 cells from 4 mice; $**p = 0.0015$). **(D)** Hierarchical clustering analysis based on Ca^{2+} responses of S1 neurons to the different textures or dynamics. Ca^{2+} responses of each cell were normalized to a single PI per each stimulus and four types of stimuli were clustered according to the PIs of cells. **(E)** Scatter plots of PIs of individual neurons for two different stimuli: (Left) Dynamic difference, F-stroke versus F-press; (Right) Texture difference, B-press versus F-press. **(F)** An example of State-space representation of population activity patterns in response to the four stimuli. N-dimensional activity patterns (N, number of cells) over time were projected onto their two or three principal components via dimensionality reduction method. Each color (yellow, light-yellow, blue and cyan) corresponds to each type of the stimuli. Black dots indicate states before stimuli onset and grey dots indicate states of inter-stimuli time. **(G)** Mean Euclidean distances between states in the state-space represented in (F). Distances were calculated between states that differ in dynamics (F-stroke versus F-press and B-stroke versus B-press, 8.308 ± 0.014), and texture (B-stroke versus F-stroke and B-press versus F-press, 9.910 ± 0.014). Data are represented as mean ± s.e.m (97,886 pairs from four mice). Statistics was performed with a two-tailed unpaired *t*-test (t = 81.71; $***p < 0.0001$).

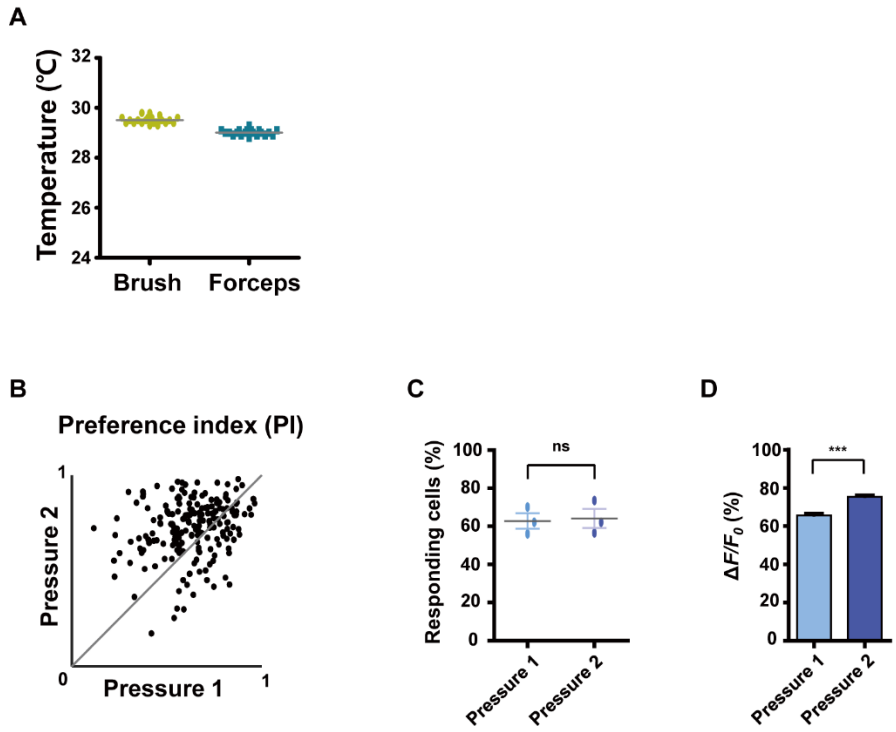

Figure 4| Effects of the temperature and indentation depth of the skin caused by the stimuli with the brush and forceps

(A) Surface temperature of brush and forceps measured by an infrared thermometer (Brush, 29.51° C ± 0.14° C; forceps, 29.01° C ± 0.12° C). Each stimulation tool was repeatedly measured 20 times. **(B)** Scatter plots of the preference indexes (PIs) of individual neurons for two different pressure: Pressure 1 versus Pressure 2 (n = 191 cells from 3 mice). Pressure 1 and 2 corresponds to 20g and 50g, respectively. **(C)** The relationship between the number of responding cells and the stimulus pressure (N = 3 mice; Wilcoxon signed rank test, ns). **(D)** The relationship between Ca^{2+} transients amplitude and the stimulus pressure (n = 191 cells from 3 mice; Two-tailed paired t-test, $p < 0.0001$). All data are represented as mean ± s.e.m.

Encoding noxiousness/intensity features of stimuli by S1 neurons

Next, I sought to identify the encoding strategy of S1 neurons for the noxiousness feature of mechanical stimuli, to which S1 neurons appear to be widely tuned (to Press and Pinch) (Figure 2, Press-specific, 0.92%; Pinch-specific, 5.99%; Both, 13.4%)). I applied graded Forceps-pinch (F-pinch) stimuli (P0 < 2g: noxiousness = innocuous; P1 = 100g, P2 = 200g and P3 = 300g pressure: noxiousness = noxious) to the hind paw, all of which have the same texture/dynamics feature (Table 1, Table 2, Figure 5A, B). I found a various response patterns of individual neurons. Interestingly, I identified 'intensity coding neurons' in a certain amount of the imaged cells (Figure $5B_i$, 21.93%), which show a positive correlation of Ca^{2+} amplitude with the stimulus intensity. Some other neurons (Figure $5B_{ii}$, 15.30%) exhibited similar amplitudes of Ca^{2+} responses to the stimuli with 4 different intensities, but the neurons showing P0 (innocuous)-preference or inverse correlation of their Ca^{2+} amplitude with the stimulus intensity were rarely detected (Figure $5B_{iii}$, 1.53%). The remaining neurons (61.24%) showed irregular patterns of Ca^{2+} responses to the stimuli with different intensities (Figure $5B_{iv}$). The positive relationship between the stimulus intensity and the proportion of responding cells was observed in a

non-linear fashion with steep and gentle slopes (N = 6 mice, **Figure 5C**). I also found such a non-linear positive relationship between the stimulus intensity and the average response fidelity (**Figure 5D**) or amplitude (**Figure 5E**) of S1 neurons, which are reflected in the response indexes (RIs; see Materials and Methods) of individual cells in response to the graded F-pinch stimuli (n = 197 cells from 6 mice, **Figure 5F**). These results suggest that the stronger the stimuli, the more S1 neurons are recruited, evoking stronger Ca^{2+} responses represented by higher amplitude and fidelity.

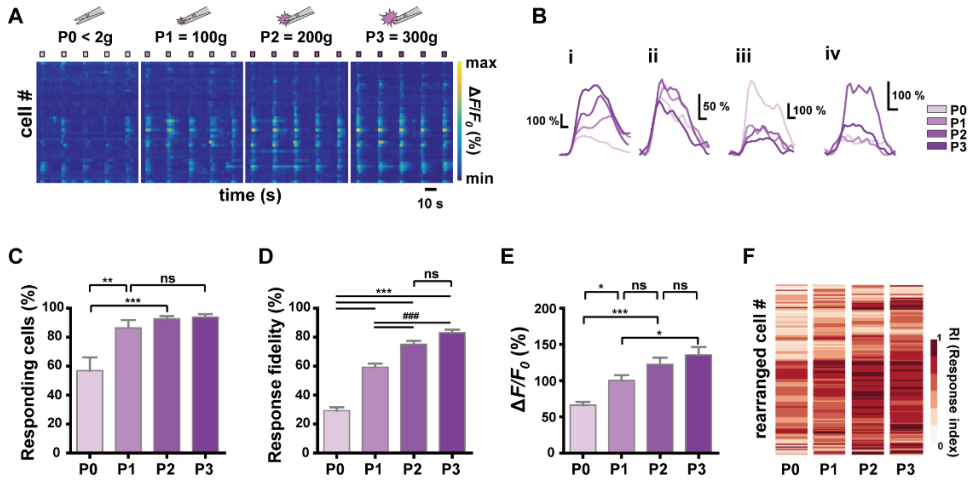

Figure 5 | Relationship between stimulus intensity and Ca^{2+} responses of S1 neurons

(A) Color-coded raster plots of representative Ca^{2+} transients in S1 neurons in response to the four different intensities (P0<2 g, P1=100±30g, P2=200±30 g and P3=300±30 g pressure). Each type of stimuli was applied 5 trials for 3s. Color-coded $\Delta F/F_0$ (%) ranges from 0 to 1000. Time scale, 10s. **(B)** Examples of various Ca^{2+} responses from four neurons to the graded pinch stimuli. Time scale, 1s. **(C)** The relationship between the number of responding cells and the stimulus intensity (N = 6 mice; one-way ANOVA, F = 10.16; p = 0.0003). **(D)** The relationship between the response fidelity of neurons and the stimulus intensity (n = 197 cells from 6 mice; one-way ANOVA, F = 104; $p < 0.0001$). **(E)** The relationship between Ca^{2+} transients amplitude and the stimulus intensity (n = 197 cells from 6 mice; one-way ANOVA, F = 13.54; $p < 0.0001$). Data are represented as mean ± s.e.m. One-way ANOVA test was performed with Tukey's post-hoc for multiple comparisons. $*p < 0.05$, $**p < 0.01$, *** and $^{###}p < 0.001$. **(F)** Heat maps from the response indexes (RIs) of cells to the stimuli with different intensities (P0, P1, P2, and P3). Cells (rows) are rearranged for the purpose of visualization (n = 197 cells from N = 6 mice).

Differential selectivity of S1 neurons to multiple stimulus features of brushing and pinch

The results so far indicated that S1 neurons have different levels of selectivity for the given stimuli with different features. To more clearly determine selectivity properties of S1 neurons for multiple stimulus features of the stimuli, I reanalyzed the obtained data in Figures 2 and 3 using only non-broadly tuned neurons (i.e. neurons with selectivity to specific features), except for neurons that were tuned to all types of stimuli. PI scatter plots of non-broadly tuned neurons were generated between two stimuli with only a single difference of features- noxiousness, dynamics, or texture (n = 101 cells from 6 mice, Figure 6A). It turned out that a certain amount of individual S1 neurons show highly specific response to the difference in texture, but low specificity to the difference in dynamics or noxiousness. Between the latter two features, neurons were slightly more specific to dynamics than noxiousness. Indeed, the average z-distance between PIs and "equally tuned" lines (grey line) for pairs of stimuli were significantly positive only in the discrimination of texture, meaning the non-broadly tuned neurons tend to be exclusive in texture coding compared to corresponding null model (Figure 6B, see Materials and Methods).

Decoding features using the response patterns of the population activity

Finally, I tried to decode the difference between the stimuli of noxiousness, dynamics, and texture using the response patterns of the population activity, rather than individual cells. K-nearest neighbor classifier achieved perfect performance in 10-fold cross validation in all the discrimination task-difference in noxiousness, dynamics, and texture (Figure 6C, see Methods). This result suggests that the information of sensory stimuli can be efficiently represented in S1 as patterns of the population, particularly in the case of low specificity to the stimuli features, such as noxiousness and dynamics.

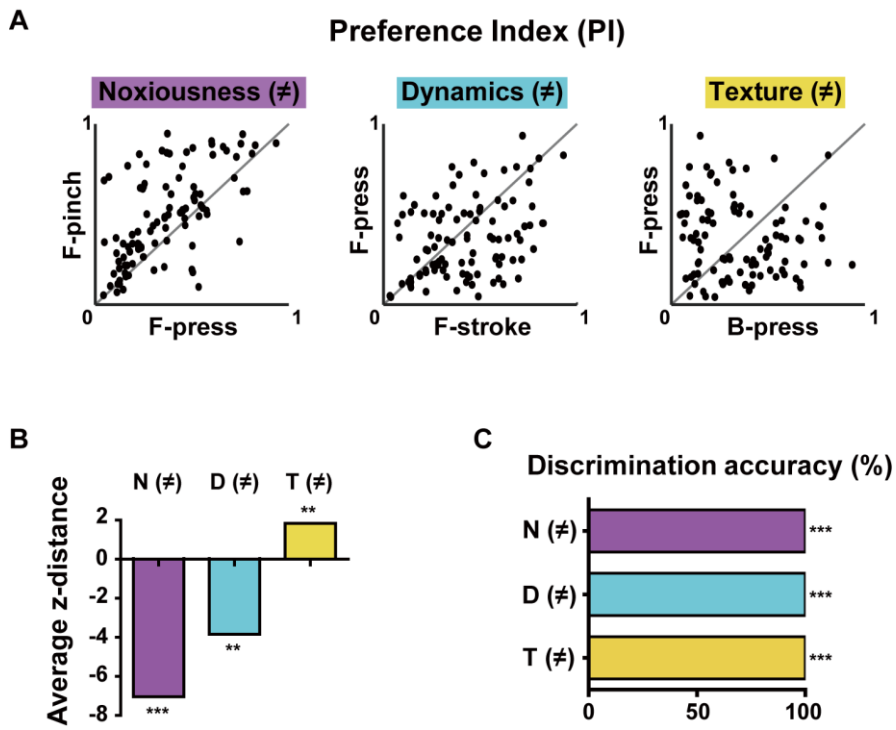

Figure 6 | Differential selectivity to multiple stimulus features and decoding features of the population activity in the S1 cortex

(A) PI scatter plots of non−broadly tuned neurons between two stimuli that differ in noxiousness (F−press versus F−pinch), dynamics (F−stroke versus F−press), or texture (B−press versus F−press) (n = 101 cells from 6 mice). Noxiousness (M)−purple, Dynamics (D)−cyan and Texture (T)−yellow. (B) Average z−distances between PIs (i.e. tuning property) and "equally tuned" lines for pairs of stimuli. Empirical p−values were calculated by permutation tests (average z−distance = −7.076, $***p < 0.001$ for F−press & F−pinch, average z−distance = −3.905, $**p < 0.01$ for F−stroke & F−press, average z−distance = 1.885, $**p < 0.01$ for B−press & F−press; Bonferroni−corrected). (C) Decoding performance for stimuli that differ in noxiousness (F−press versus F−pinch), dynamics (F−stroke versus F−press), or texture (B−press versus F−press) by neural population activity ($***p < 0.001$).

DISCUSSION

S1 integrates sensory information from diverse afferent sources, leading to perception of the location, intensity, quality of touch, a nd pain (Vierck et al., 2013). However, little is known how the neural circuits in S1 inclusively process such various features at the single-cell and population levels. In this study, I determined how diverse features of cutaneous inputs are encoded in layer 2/3 S1 cortex of the mouse. I found that different aspects of the stimuli are encoded with different levels of selectivity at the individual neuron level. Under the stimuli conditions given here, texture was the most dominant feature that was selectively encoded at the single-cell level, followed by dynamics, and noxiousness. However, it turned out that the stimulus features with low neuronal selectivity can be successfully decoded by the supervised machine learning technique, implying the distributed information encoding of such features. These findings suggest that S1 neurons encode multiple stimulus features of touch and pain at the individual cell and population levels in a feature-dependent manner.

Primary somatosensory afferents, such as LT mechanoreceptors and HT nociceptors, are specifically tuned to innocuous or noxious mechanical stimuli (Prescott et al., 2014; Zimmerman et al., 2014). This “specificity” or “labeled line” tuning in the periphery, however,

cannot be simply applied to the CNS neural circuits. Even in the spinal cord that receives direct inputs from primary afferents, LT, HT and WDR neurons coexist (Price et al., 2003; Sekiguchi et al., 2016). These differentially classified neurons structurally and functionally interact in the spinal cord and thalamus, and further in the S1 cortex (Craig, 2003; Price et al., 2003; Basbaum et al., 2009), leading to a long "specificity" versus "pattern" debate (Craig, 2003; Perl, 2007; Prescott et al., 2014). This study demonstrates a mixed specificity and pattern coding of touch and pain mechanosensations in the mouse S1 cortex, i.e. stimulus feature–dependent distinct response patterns of neural population and hierarchical specificity of individual cells (schematically summarized in **Fig 7**). Thus, when we categorize the somatosensory neurons into LT, HT and WDR, the qualitatively different stimulus features also need to be considered.

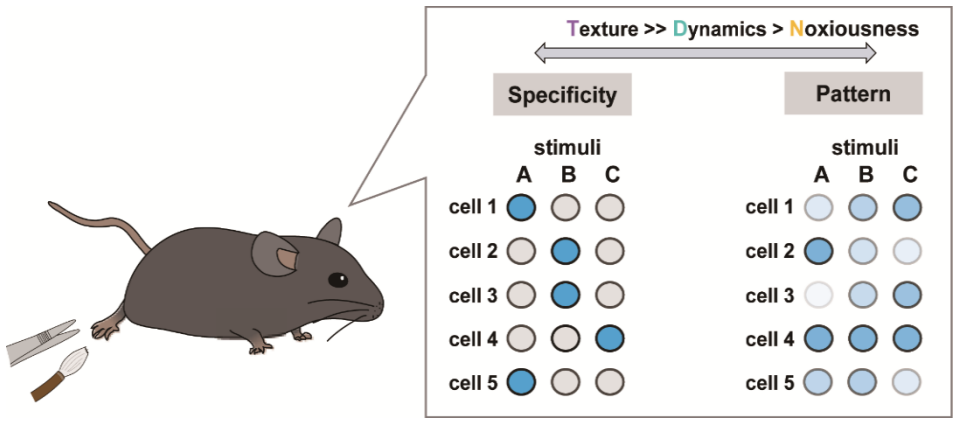

Figure 7| Schematic diagram for specificity versus pattern coding theory
In specificity theory, each stimulus is encoded by individual neurons that are selectively responsive to a specific stimulus. While in pattern theory, each stimulus is encoded by the composite pattern of activity in the neural population. My findings reveal differential S1 neural population responses with a hierarchical selectivity of individual cells to multiple stimulus features of touch and pain (i.e. texture >> dynamics > noxiousness).

Previous electrophysiological studies characterizing S1 neurons for noxiousness in animals demonstrated that the proportion of nociceptive specific HT neurons is much smaller than that of non-nociceptive LT and convergent WDR neurons (Lamour et al., 1983; Kenshalo et al., 2000). These results also showed that a majority of S1 neurons responded to non-nociceptive brushing/press stimuli and exhibited highly selective responses toward non-nociceptive texture features derived from a brush or a forceps steel arm. Previous *in vivo* studies of S1 barrel cortex have reported that layer 2/3 neurons

show preferred response patterns to specific texture coarseness, while a minority of neurons responds monotonically to the graded texture coarseness (Garion et al., 2014; Bourgeon et al., 2016). Taken together, these results imply that texture features of tactile information are well discriminated at the individual cell level in S1.

Discrimination of different tactile features is associated with Merkel cells and Meissner's corpuscles at peripheral level. Traditionally, cutaneous sensory information is thought to be conveyed from peripheries to the cortex via independent neural pathways according to their submodality, which is characterized by response properties of afferent classes; rapidly adapting (RA), slowly adapting type 1 (SA 1), slowly adapting type 2 (SA 2), and Pacinian (PC) afferents. Representations of static (slowly adapting) and dynamic (rapidly adapting) inputs from Merkel cells and Meissner's corpuscles, respectively, are segregated in a columnar fashion in the primate S1 cortex (Paul et al., 1972; Sur et al., 1984). However, optical imaging approaches have proposed another possibility that some cortical columns could be overlapped by slowly adapting and rapidly adapting inputs (Johnson and Lajtha, 2007). In addition, recent evidence shows that individual neurons in S1 receive inputs from multiple afferent classes, and therefore should not be defined based on submodality, but on their function (Saal and

Bensmaia, 2014). These reports are consistent with my results; about half of the analyzed neurons responded to both dynamic and static stimuli, implying that the dynamics feature is multiplexed at the single-cell level. However, the stimuli frequency difference between the given stimuli in the dynamics feature experiments was less than 1 Hz. This may not be sufficient to excite different mechanoreceptors at the periphery. I preliminary investigated whether the S1 neurons exhibit selective responses by giving two different frequency (Hz) stimuli. These two frequency stimuli are sufficiently different to stimulate different mechanoreceptors at the periphery. I recorded Ca^{2+} activities of S1 neurons while applying static touch stimuli (<1 Hz) or dynamic stimuli with 150 Hz of vibrations. Unlike the results of the dynamics feature experiments, S1 neurons showed selective responses to static touch (<1 Hz) or dynamic stimuli (150 Hz) (**Figure 8A and 8B**). It is generally accepted that Merkel cells, Meissner's corpuscle, and Pacinian corpuscle are activated by <2Hz, 2~40Hz, and 40~200Hz, respectively (Johansson et al., 1982). Further studies, through applying stimuli that activate different mechanoreceptors at periphery, are needed to determine whether segregation by each type of mechanoreceptors responsible for different functions is preserved from periphery to the S1 cortex.

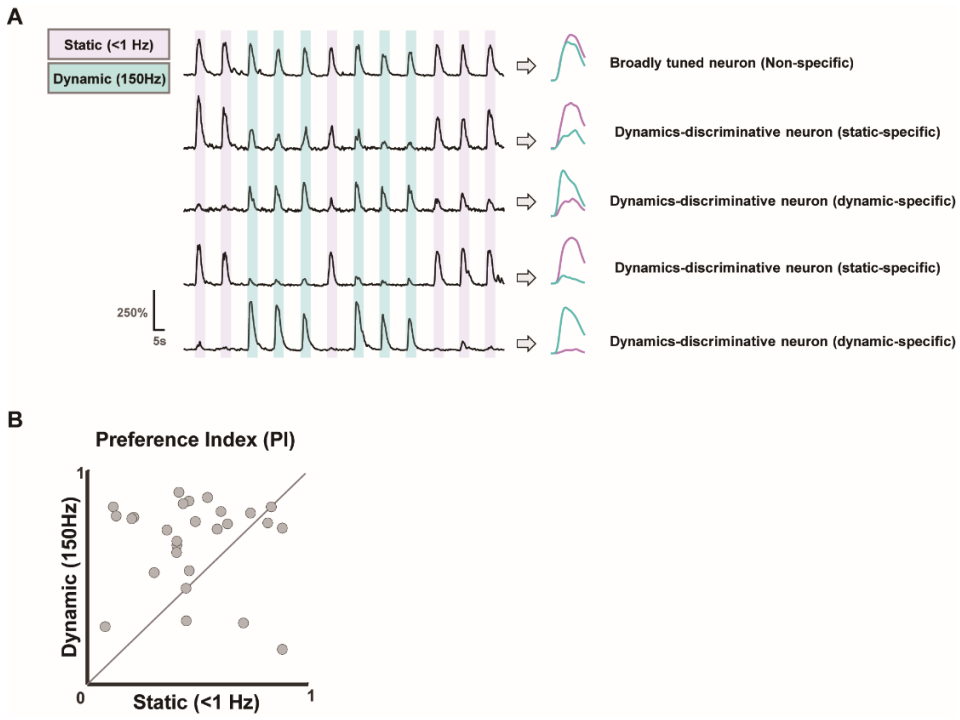

Figure 8| Selective responses of S1 neurons evoked by different stimulus frequency

(A) Representative Ca^{2+} transients of S1 neurons in response to static (< 1Hz) and dynamic (150Hz) stimuli. Each stimulus was randomly applied six trials for 5 seconds. Purple (static) and green (dynamic) vertical lines represent the stimulus period. The traces on the right side of each trace are the average of the responses to each stimulus given 6 trials. Purple and green correspond to static and dynamic stimulation, respectively. **(B)** Scatter plots of preference indexes (PIs) of individual neurons for the two different stimuli: Static (<1 Hz) versus Dynamic (150 Hz).

My study also examined how different pain intensities are represented in the S1 neurons. Previous pain studies, mainly examined in the spinal cord and thalamus, have investigated how noxiousness feature is represented in somatosensory neurons using brush or forceps pinch to apply the innocuous or noxious stimulus, respectively, to the animals (Light et al., 1979; Lamour et al., 1983; Apkarian and Shi, 1994). However, the brush and forceps pinch that were used as innocuous or noxious stimulation have mixed characteristics in noxiousness (strong/weak) and quality (textures/dynamics) features. In this study, I observed response of S1 neurons to the noxiousness/intensity feature by applying graded F-pinch stimuli with the same Texture/Dynamics feature but only with different intensities. Most of neurons exhibited irregular or broadly tuned responses to the graded F-pinch stimuli. At the population level, however, I found that more S1 neurons are recruited and stronger Ca^{2+} responses are evoked as the stimulus intensity is increased in a nonlinear manner. This result agrees with the previous studies showing that the stimulation intensity is positively correlated with S1 neuronal responses in a nonlinear fashion (Timmermann et al., 2001; Bornhovd et al., 2002; Eto et al., 2011). Since S1 neurons showed low selectivity towards noxiousness features, I investigated whether the responses of S1 neurons to noxious range of graded F-

pinch stimuli are selectively reduced when nociceptors are selectively blocked at the periphery (**Figure 9**). I recorded Ca^{2+} activities of S1 neurons after applying saline into the right hind paw of mice. Two days after the first imaging was performed, I repeatedly imaged the same neurons after co-applying QX-314 and capsaicin, or applying saline alone into the right hind paw of mice (Kim et al., 2010). Most of the S1 neurons showed similar responses to graded F-pinch stimuli when saline was injected (**Figure 9A**). However, when nociceptors were selectively blocked at periphery, Ca^{2+} activities of S1 neurons to graded F-pinch stimuli were generally reduced (**Figure 9B**). Unlike my expectation that selective nociceptor blockade will only affect the responses to noxious range of the stimuli, some neurons showed reduced Ca^{2+} responses to innocuous P0 stimuli as well as noxious P1-3 stimuli. Few neurons even showed an increased response towards stimuli after a selective nociceptor blockade. These results imply that the effect of nociceptor blockade could be different for each cell type. Future research will be a clarification of how these each type of neurons with distinct functional properties are involved in pain processing.

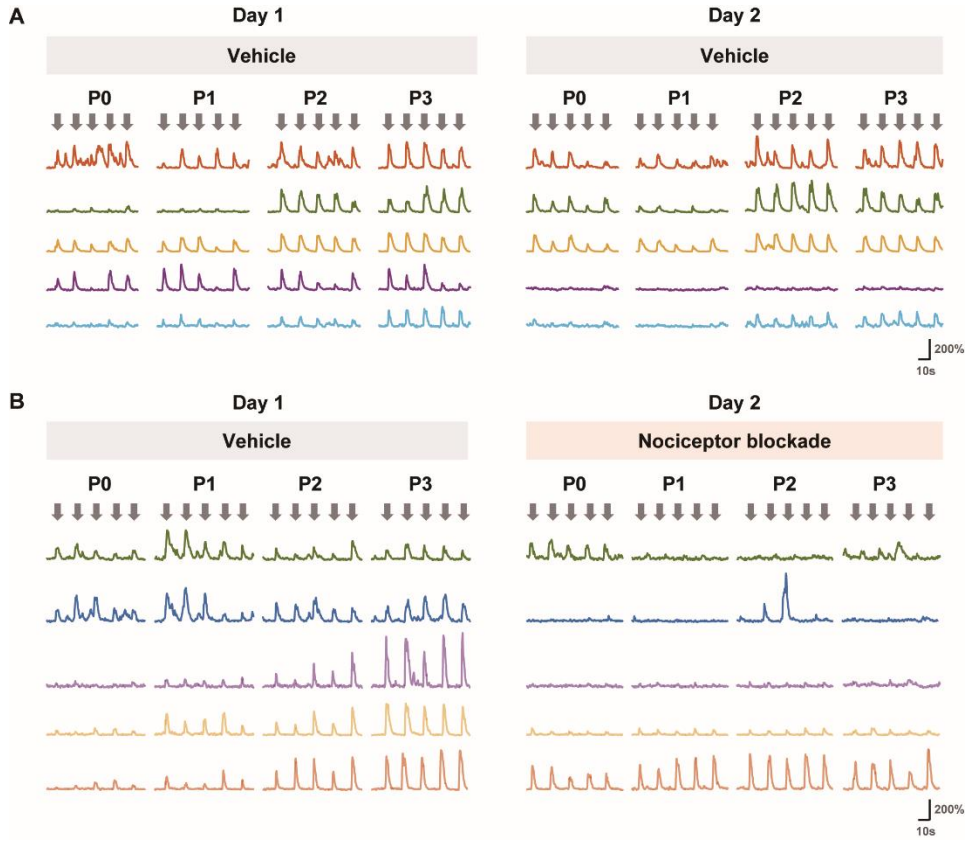

Figure 9| Effects of selective nociceptors blockade on S1 neurons to innocuous and noxious stimuli.

(A, B) Representative Ca^{2+} transients of S1 neurons to graded F-pinch stimuli, repeatedly recorded after injection of vehicle or nociceptor blocker (day2). Each arrow represents the stimulation time points. Each type of stimuli was applied 5 trials for 3s (P0<2 g, P1=100±30g, P2=200±30 g and P3=300±30 g pressure).

In this study, a majority of S1 neurons responded to more than two types of stimuli, rather than selectively responded to each texture, dynamics or noxiousness, indicating that individual S1 neurons encode multiple features of sensory information. Given the multifaceted nature of the sensory information in real life setting, this is a reasonable and efficient strategy to process numerous types of distinct stimuli within a limited sensory system resources (Chu et al., 2016). Indeed, similar phenomena have been reported in complex cognitive tasks of the prefrontal cortex, known as 'mixed selectivity' (Rigotti et al., 2013; Ramirez-Cardenas and Viswanathan, 2016; Parthasarathy et al., 2017). Thus, these findings extend this 'mixed selectivity' concept to the somatosensory cortex, suggesting that it is more general mechanism in the cortex than previously thought.

A limitation of my study is worth mentioning. All the experiments in this study were performed under isoflurane anesthesia. The anesthesia was inevitable since it is extremely difficult to repeatedly stimulate the same regions in awake animals and to control other sensory inputs from movements. It has been shown that the anesthesia reduces tuning properties of neurons to stimuli in the V1 and A1 cortex of rodents (Gaese and Ostwald, 2001; Goltstein et al., 2015). Thus, I cannot completely rule out the possibility that the evoked responses of the neurons are influenced by the isoflurane

anesthesia, although it is unlikely that such changes will appear in a feature-dependent manner.

In conclusion, I demonstrated the differential selectivity of S1 neurons for multiple stimulus features of touch and pain. The majority of tuned neurons selectively responded to texture features rather than noxiousness features, implying that conventional classification of neurons (LT, HT, and WDR) in pain studies cannot be simply employed in the S1 cortex. Sensory stimuli could be decoded via patterns of neural population activity, even for the features with low specificity at the individual cell level. I also showed a group of neurons in the S1 cortex encodes pain intensity by amplitude and fidelity. These results provide an important insight into the encoding strategy of S1 neural circuits for multiple stimulus features of touch and pain.

Chapter 2

Alterations in response properties of S1 neurons to innocuous and noxious stimuli in CFA-induced hypersensitivity

Introduction

The role of primary somatosensory cortex (S1) is to process sensory-discriminative aspects of non-painful and painful stimulation (Bushnell et al., 1999; Basbaum et al., 2009). Tissue or nerve injury can lead to a chronic pain such as inflammatory or neuropathic pain (Woolf et al., 2004). In tissue/nerve injured chronic pain models, it has been reported that structural and functional plastic changes occurred in pain matrix including primary somatosensory cortex and the functional connectivity between the regions are modified (Eto et al., 2011; Kim and Nabekura, 2011; Kim et al., 2014). Previous *in vivo* studies of S1 cortex have also demonstrated that spontaneous activity of layer II/III and IV neurons and response to peripheral stimulation increased in the chronic pain models (Eto et al., 2011; Cichon et al., 2017).

Chronic pain is usually associated with hypersensitivity such as allodynia and hyperalgesia. In neuropathic pain or inflammatory pain models, subject animals showed a decreased pain threshold and became hypersensitive to sensory stimuli (Costigan et al., 2009). There are two types of hypersensitivity: Allodynia is a pain caused by non-painful stimuli such as gentle bush of the skin, while hyperalgesia shows enhanced pain responses to normal pain

stimulus. Little is known which types of S1 neurons are associated with hypersensitivity and which response property change of the S1 neurons causes these abnormal pain sensitivities.

Here, I investigated how response properties of S1 neurons are changed in hypersensitivity and which types of neurons contribute to pain hypersensitivity in S1. In this study, Complete Freund's Adjuvant (CFA) was injected into the right hind paw of mice to generate hypersensitivity (Kopach et al., 2012). Using *in vivo* two-photon Ca^{2+} imaging, I found that the response tuning properties of noxious-preferred neurons were changed when the hypersensitivity is generated by CFA. Broadly tuned neurons, which responded to both innocuous and noxious stimuli at normal states, however, did not show an altered tuning property during CFA-induced hypersensitivity. Instead, these neural population showed increased responses to the mechanical stimuli in hypersensitivity state. These findings provide important information regards how each type of neurons in S1 cortex differentially contributes to the hypersensitivity.

Results

Mechanical hypersensitivity induced by Complete Freund's adjuvant (CFA) administration in mice

Prior to generate hypersensitivity, paw withdrawal test was performed in mouse to establish mechanical thresholds. Mice were injected with 10uL of CFA into the right hind paw to generate mechanical hypersensitivity (Figure 10A). Two days after saline or CFA administration, paw withdrawal test was repeatedly performed (Figure 10B). In CFA-injected animals, paw withdrawal threshold was significantly reduced compared to that of control group (Figure 10C), which indicates that CFA administration successfully induced mechanical hypersensitivity.

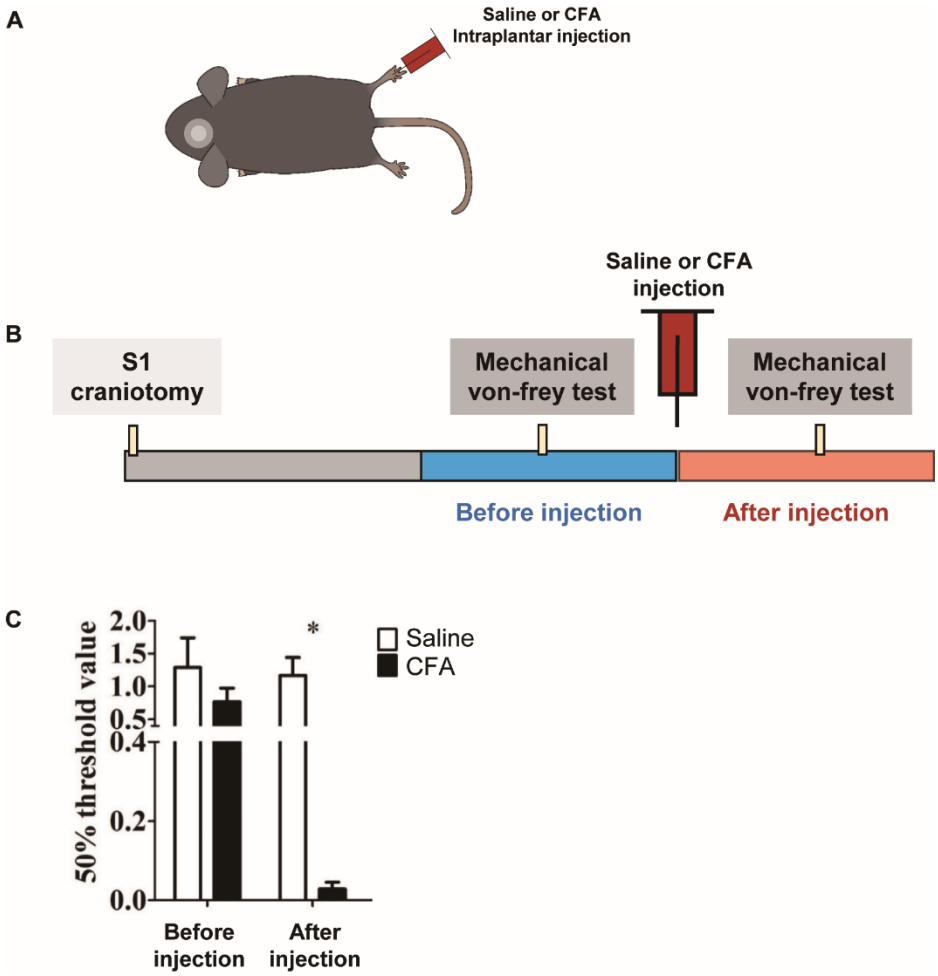

Figure 10| Experimental design of paw withdrawal test

(A) Mice received an intraplantar injection of saline or CFA in the right hind paw. (B) Two weeks after S1 craniotomy, mechanical threshold was evaluated repeatedly before and after injection of CFA (or saline). (C) Paw withdrawal threshold was significantly decreased in the CFA-injected group compared to the control.

Response properties of S1 neurons to innocuous and noxious stimuli in CFA-induced hypersensitivity

I investigated how response properties of S1 neurons towards an innocuous and noxious mechanical stimulus change in CFA-induced hypersensitivity compared to a normal state. Using *in vivo* two-photon Ca^{2+} imaging, I repeatedly recorded Ca^{2+} activities of the same neurons in layer 2/3 of S1 cortex before and after CFA administration while applying innocuous touch and noxious pinch stimuli to the right hind paw (Figure 11). Since the mechanical hypersensitivity occurred two days after CFA injection, which is demonstrated by a significantly reduced paw withdrawal threshold, next Ca^{2+} imaging was performed 2 days after CFA injection. When the imaging was repeated under normal and CFA-induced pain states with 2-day intervals, most neurons were remained active in response to mechanical stimuli. I investigated whether there is a change in response properties of S1 neurons to innocuous touch and noxious pinch stimuli in CFA-induced hypersensitivity compared with a normal state. About a third of the responding neurons (38.29%) showed no change in response to innocuous and noxious mechanical stimuli in CFA-induced hypersensitivity compared to normal state (Figure 12A). The majority of the neurons responded to both types of stimuli at normal state and maintained similar response properties

in CFA-induced hypersensitivity. More than half of the responding neurons, however, showed changes in the Ca^{2+} responses to innocuous touch and noxious pinch stimuli in CFA-induced hypersensitivity. Next, I examined whether response tuning property of S1 neurons have changed in response to innocuous and noxious stimuli in CFA-induced hypersensitivity. Approximately one-third of responding neurons showed changes in the Ca^{2+} responses and their tuning properties to innocuous and noxious stimuli (**Figure 12A-C**). The majority of those neurons were noxious-preferred neurons (81.26%), which previously responded to noxious pinch stimuli dominantly in normal states but switched themselves to broadly tuned neurons or innocuous-preferred neurons in CFA-induced hypersensitivity. However, in CFA-induced hypersensitivity, there are some neurons that only changed the Ca^{2+} response amplitude without altering the tuning properties to the stimuli (**Figure 12A-C**). Most (90.94%) of them were broadly tuned neurons that responded to both innocuous and noxious mechanical stimuli. The response amplitude to innocuous touch and noxious pinch stimuli was increased in these neurons, while the other minor neuronal population showed a decreased Ca^{2+} response amplitude in CFA-induced hypersensitivity. The total amplitude of the Ca^{2+} response of all neurons was increased for both innocuous and noxious stimuli in the

CFA-induced hypersensitivity compared to the normal state. The response amplitude of neurons with unchanged tuning property also increased for both types of stimuli in CFA-induced hypersensitivity compared to normal state. (Figure 12D). However, there was no significant difference between the response amplitude of the normal state and that of the CFA-induced hypersensitivity. I also found that only a small number of neurons (4.26%) did not respond to mechanical stimuli in the normal state, but were newly recruited giving novel responses to the stimuli in the hypersensitivity (Figure 12A-C). Taken together, noxious-preferred neurons that responded to predominantly noxious pinch stimuli at normal state were altered their tuning properties in CFA-induced hypersensitivity. Broadly tuned neurons, however, showed increased responses to innocuous and noxious mechanical stimuli while maintaining their tuning properties to the stimuli in CFA-induced hypersensitivity.

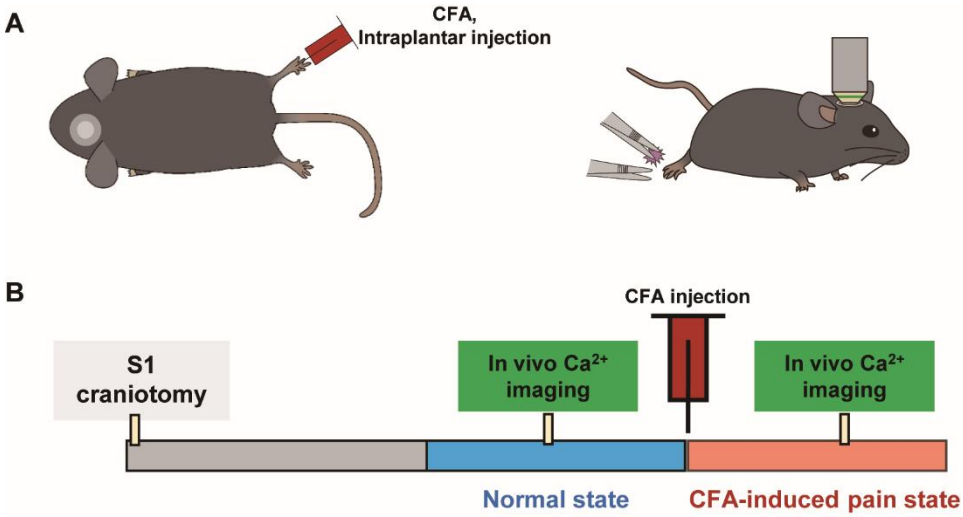

Figure 11| Experimental design and *in vivo* Ca^{2+} imaging schedule

(A) Mice received an intraplantar injection of CFA in the right hind paw after finishing the first imaging session (normal states). Innocuous touch and noxious pinch stimuli were applied while S1 neurons were recorded. **(B)** Two weeks after S1 craniotomy, *in vivo* Ca^{2+} imaging was performed repeatedly before (normal states) and after injection of CFA (CFA-induced pain states).

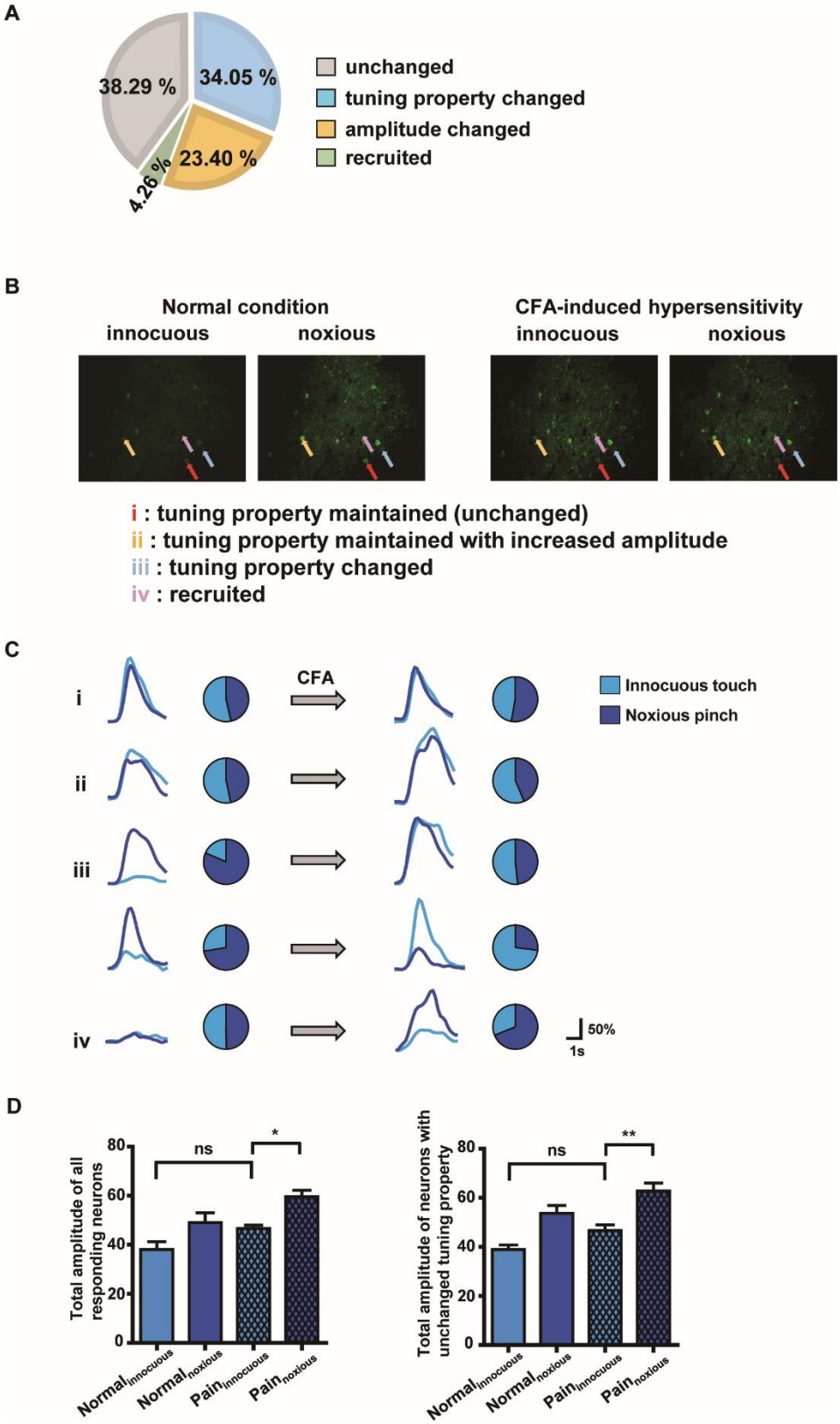
A
38.29 %
34.05 %
23.40 %
4.26 %
unchanged
tuning property changed
amplitude changed
recruited
B
Normal condition
innocuous
noxious
CFA-induced hypersensitivity
innocuous
noxious
i : tuning property maintained (unchanged)
ii : tuning property maintained with increased amplitude
iii : tuning property changed
iv : recruited
C
CFA
Innocuous touch
Noxious pinch
i
ii
iii
iv
50%
1s
D
Total amplitude of all responding neurons
ns
*
Normal innocuous
Normal noxious
Pain innocuous
Pain noxious
Total amplitude of neurons with unchanged tuning property
ns
**
Normal innocuous
Normal noxious
Pain innocuous
Pain noxious

Figure 12| Response properties of S1 neurons to innocuous and noxious mechanical stimuli in normal states and CFA-induced hypersensitivity.
(A) Pie chart indicating proportions of response patterns in CFA-induced hypersensitivity compared to the control (normal states). Grey-unchanged, light blue-tuning property changed, yellow-Ca^{2+} response amplitude changed and green-newly recruited. **(B)** Representative imaging field in normal conditions and CFA-induced hypersensitivity. Four arrows indicate representative response patterns in normal states and CFA-induced hypersensitivity. Red-tuning property maintained, yellow-tuning property maintained with increased amplitude, light blue-tuning property changed and light purple-newly recruited. **(C)** Representative traces of S1 neurons to innocuous touch and noxious pinch stimuli before (normal states) and after CFA injection (CFA-induced hypersensitivity). Each trace is the averaged trace of the responses to each stimulus given 5 trials. Sky blue and deep blue correspond to innocuous touch and noxious pinch stimuli, respectively. **(D)** Total amplitude of all responding neurons (left) and neurons with unchanged tuning property (right) in normal states or CFA-induced hypersensitivity, in response to innocuous touch or noxious pinch. Data are represented as mean ± s.e.m. One-way ANOVA test was performed with Tukey's post-hoc for multiple comparisons. $*p < 0.05$, $**p < 0.01$.

Discussion

I investigated how the response properties of S1 neurons to innocuous and noxious mechanical stimuli change in CFA-induced hypersensitivity. A significantly decreased paw withdrawal threshold, compared to control, demonstrated that mechanical hypersensitivity was successfully induced by CFA administration. Using *in vivo* two-photon Ca^{2+} imaging, I found that response amplitude of broadly tuned neurons increased without any change in tuning properties in CFA-induced hypersensitivity. However, noxious-preferred neurons which preferentially responded to noxious pinch stimuli in normal states responded to innocuous touch stimuli in CFA-induced hypersensitivity (Figure 13). These results imply that S1 neurons involves in CFA-induced hypersensitivity by changing its tuning properties and increasing its response amplitude, rather than recruiting new neurons.

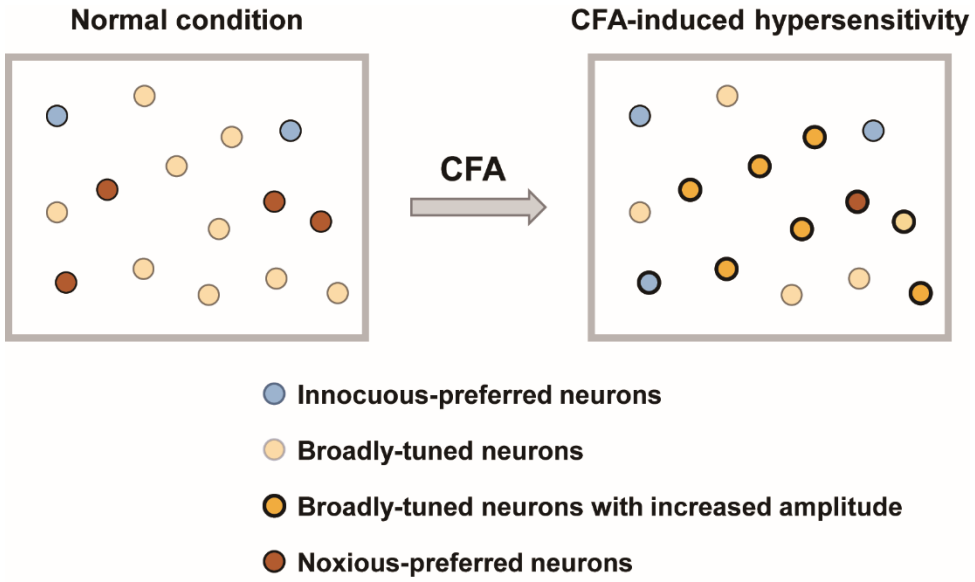

Figure 13| A diagram to illustrate the altered response properties of S1 neurons in CFA-induced hypersensitivity

Under normal conditions, S1 neurons coexist with neurons that selectively respond to innocuous or noxious stimuli and neurons that respond to both types of stimuli. After hypersensitivity is induced by CFA, some neurons show changes in response properties to innocuous and noxious mechanical stimuli. Some of the noxious-preferred neurons become respond to innocuous touch as well as noxious pinch stimuli in the CFA-induced hypersensitivity. In addition, a few of the noxious-preferred neurons respond only to innocuous touch in CFA-induced hypersensitivity, which indicates that their tuning properties are changed in CFA-induced hypersensitivity. However, a majority of broadly tuned neurons are more responsive to both innocuous and noxious stimuli without altering tuning properties in CFA-induced hypersensitivity. Taken together, S1 neurons are involved in CFA-induced hypersensitivity in a way that tuning properties are changed in noxious-preferred neurons and activities of broadly tuned neurons are generally increased.

Previous studies have shown that wide dynamic range (WDR) neurons provide important information for pain sensation not only in normal physiological conditions but also in post-injury pain states (Kenshalo et al., 2000; Hao et al., 2004; Gwak and Hulsebosch, 2011). Electrophysiological studies demonstrated that WDR neurons of spinal cord and thalamus show high sensitivity to noxious thermal stimuli in nerve- or spinal injury animals. In addition, spinal injury altered the proportion of low threshold (LT), high threshold (HT) and WDR neurons of spinal dorsal horn. The proportion of HT neurons decreased after a spinal injury but that of WDR neurons increased in bilateral sides of spinal dorsal horn after the injury compared to controls. After SCI, WDR neuronal activities on both side of thalamic VPL regions also increased (Gwak et al., 2010). These results imply that activity of WDR neurons provides a crucial information for pain processing after injury. More importantly, these reports are consistent with my experimental results. My study showed that broadly tuned neurons exhibit increased responses to the same stimuli during CFA-induced hypersensitivity. I previously reported that broadly tuned neurons of S1 cortex are mainly recruited when processing different pain intensities (Kim et al., 2019). Increased responsiveness of the broadly tuned neurons is expected to contribute significantly to hyperexcitability of the S1

cortex in injury-induced pain conditions. I also found that the majority of the broadly tuned neurons did not change their tuning properties in CFA-induced hypersensitivity, but the tuning properties of noxious-preferred neurons were changed a lot like those of broadly tuned neurons in CFA-induced hypersensitivity. This phenomenon may suggest a possibility of a novel input to noxious-preferred neurons in pain hypersensitivity. This possibility can explain why the S1 cortex is hyperexcitable to weak stimuli in allodynia compared to normal physiological conditions. A few noxious-preferred neurons' tuning properties were changed like those of innocuous-preferred neurons. This phenomenon seems impossible at the first glance, but human brain imaging and I previously found that some of the S1 neurons were less responsive or even no responsive when intensity of noxious stimuli becomes very strong (Timmermann et al., 2001; Bornhovd et al., 2002; Kim et al., 2019). Because normal painful stimuli provoke enhanced pain responses in pain hypersensitivity such as hyperalgesia (Costigan et al., 2009), decreased Ca^{2+} activities in noxious-preferred neurons to noxious stimuli in CFA-induced hypersensitivity may happen as the intensity of the given noxious pinch stimuli is exceeded the physiological range that can be normally represented by S1 neurons. As a result, the activity of some of the S1 neurons to noxious stimuli

could decrease in CFA-induced hypersensitivity. To ensure this type of neurons are associated with hyperalgesia, further experiment is essential to identify whether the response of the S1 neurons to weak pain stimuli at the hypersensitivity condition is as large as the response to the strong pain stimuli at the normal condition. In further research, I will confirm which types of neurons in the S1 cortex contribute to allodynia or hyperalgesia by examining the functional connectivity between the S1 neurons whose response properties have changed in CFA-induced hypersensitivity. It is necessary to confirm whether each type of neurons mentioned above is forming a hub in the network in mechanical hypersensitivity.

Tissue or nerve injury can lead to pain hypersensitivity such as mechanical allodynia or hyperalgesia. These abnormal pain symptoms are characteristic of neuropathic pain (Costigan et al., 2009). Previous studies have shown an increased activity of pain matrix such as ACC and S1, additional brain region recruitments, and an altered cortical thickness of S1 in nerve-injured patients or animals (Lorenz et al., 2002; Seifert and Maihofner, 2009; Gustin et al., 2012). In addition, connectivity of the pain matrix changed and the default mode network was disrupted in the neuropathic pain. Recently, brain imaging study demonstrated that the connectivity patterns of brain networks were modified and the connectivity was

increased between prefrontal, S1 and M2 cortices in neuropathic pain animal model (Kim et al., 2014). Functional and structural plastic changes occur not only in large-scale networks but individual cell levels. Using *in vivo* two-photon imaging, it is reported that structural plastic changes of individual neuronal circuits occur in S1 cortex (Kim and Nabekura, 2011). It showed the formation of new dendritic spines in the development phase of neuropathic pain and a significant increase in the size of the dendritic spines associated with synaptic strength. My study showed that response properties of S1 neurons to innocuous and noxious mechanical stimuli changed in CFA-induced hypersensitivity. The altered response properties may be due to the changed synaptic connections with surrounding neurons. If dendritic spines were newly formed under CFA-induced hypersensitivity, as in nerve-injured neuropathic pain model, the newly formed dendrites may have altered synaptic strength with neighboring neurons. As a result, it may alter the response properties of the neurons to innocuous and noxious mechanical stimuli in the CFA-induced hypersensitivity. Gabapentin (GBP) is known to prevent excitatory CNS synaptogenesis and recently used as a drug to relieve neuropathic pain symptoms (Eroglu et al., 2009; Alles et al., 2017). GBP attenuated hypersensitivity in animal model within 30min of an intraperitoneal (IP) injection. Electrophysiological and

imaging studies demonstrated that S1 neurons as well as spinal cord neurons obtained ex vivo from GBP-injected neuropathic pain animals did not display increased excitability. If the gabapentin is directly applied into the S1 cortex and the observed changes in CFA-induced hypersensitivity are blocked, we can confirm that S1 cortex plays a leading role in CFA-induced hypersensitivity, not just reflecting the phenomenon occurring in the periphery or spinal cord.

Materials and Methods

Animal preparation and virus injection

All experimental procedures were approved by the Seoul National University Institutional Animal Care and Use Committee and performed in accordance with the guidelines of the National Institutes of Health. I used C57BL/6 male mice (5−6 weeks old at the surgery). All surgeries were conducted under isoflurane anesthesia (1−1.5%). A cranial window was made over the left S1 cortex hind paw area (size, 2x2mm; center relative to Bregma: lateral, 1.5; posterior 0.5mm) (Eto et al., 2011; Kim and Nabekura, 2011). The animal skull was opened above the S1 cortex and a small craniotomy was carefully performed using a #11 surgical blade (Jin et al., 2016). The dura was left intact. This exposed cortex was super fused with ACSF. And I injected adeno−associated virus expressing GCaMP6s (AV−1−PV2824; produced by University of Pennsylvania Gene Therapy Program Vector Core) into the S1 cortex at 2−4 sites (30−50 nl per site; 200−300 μm from the surface) using a broken glass electrode (20−40 μm tip diameter). Finally, the exposed cortex was covered with a thin cover glass (Matsunami, Japan) and the margin between the skull and the cover glass was tightly sealed with Vetbond (3M). Mouse body temperature was maintained at 36~38° C using a heating pad (IL−H−80, Live Cell Instrument) during animal surgery

and imaging experiments. Dexamethasone (0.2 mg/kg) and meloxicam (20 mg/kg) were administered by subcutaneous injection prior to surgery to minimize the potential edema and inflammation (Otazu et al., 2015; Jin et al., 2016). Imaging sessions started 2 weeks after the surgery. Only two mice were housed in each cage in the vivarium to minimize stress on each other. The vivarium was controlled with 12 hr light/dark cycle and all experiments were performed during the daylight hours.

Animal model: CFA-induced hypersensitivity

To generate CFA-induced hypersensitivity, 10uL of CFA (or vehicle) was injected subcutaneously into the right hind paw (Eto et al., 2011; Kopach et al., 2012). Two days later, paw withdrawal test or *in vivo* Calcium imaging were performed.

Behavioral test: Paw withdrawal threshold

The mechanical threshold was evaluated using von Frey filaments as previously described (Dixon, 1965, Chanplan et al., 1994, Chen et al., 2010). Briefly, mice were individually acclimated in individual transparent acryl cage on a metal mesh floor table for 30 mins prior to testing. The right hind paw was touched with a series of von Frey filaments until a withdrawal response noted. 50% paw withdrawal

threshold was calculated by up-down paradigm (Dixon 1980, Chaplan et al., 1994).

Chemicals: Selective nociceptor blockade

For selective C-fibers blockade, QX-314 (0.2%, 10 μL) and capsaicin (0.1%, 10 μL) are co-applied via intraplantar injection into the right hind paw of the mice (Kim et al., 2010). Saline was injected as a control. Capsaicin was dissolved in 80% saline, 10% ethanol and 10% Tween 80 solution. QX-314 was dissolved in saline.

Peripheral stimulation during imaging experiments

All stimuli were delivered to the right hind paw using brush or stainless forceps. For texture and dynamics features experiment (N = 4 mice, Figure 3), brush and forceps stimuli were subdivided into Brush-stroke (B-stroke, 1-Hz stroke by brush), Brush-press (B-press, light press by brush), Forceps-stroke (F-stroke, stroke by forceps) and Forceps-press (F-press, < 2 g light press by forceps) according to their texture and dynamics (Table 1, Table 2). Stimuli were applied for 5 s per stimulus and inter-stimulus intervals were 15~20 s to avoid sensitization. For aversive noxiousness and intensity experiment (N = 6 mice, Figure 5), pinch stimuli were delivered by the experimenter using a rodent pincher meter [Rodent

pincher, BIOSEB] for 3 s per stimulus to minimize sensitization (F-pinch) (Poisbeau et al., 2005). Inter-stimulus intervals were 20 s and stimulation intensities were P0 < 2 g, P1 = 100g, P2 = 200g and P3 = 300g. The intensities were manually controlled by the experimenter (Kim et al., 2016). For hypersensitivity experiment (N = 4 mice, Figure 12), innocuous touch and noxious pinch were applied with stainless forceps for 3s per stimulus.

In *vivo* two-photon calcium imaging of layer 2/3 neurons

Calcium imaging was performed with a two-photon microscope (Zeiss LSM 7 MP, Carl Zeiss, Jena, Germany) equipped with a water immersion objective (Apochromat 20x, NA = 1.0, Carl Zeiss). Two-photon excitation for GCaMP6s imaging (900 nm) was provided by a mode locked Ti: sapphire laser system (Chameleon, Coherent). Imaging was acquired using ZEN software (Zeiss Efficient Navigation, Carl Zeiss). All the experiments were conducted under anesthesia with isoflurane (1%) and the body temperatures of mice were maintained at 36~38° C using a heating pad (IL-H-80, Live Cell Instrument). For layer 2/3 neurons calcium imaging, time-lapse imaging (512x300 pixels, 0.4 μm/pixel, 2 line steps, 0.229 s per frame) was performed with imaging depth of 180~220 μm from the surface.

Data analysis

I manually selected regions of interest (ROIs) corresponding to individual neurons by circling each fluorescence, using time-lapse movie program. Customized scripts in MATLAB were used to analyze the calcium transient signals. Calcium signal amplitudes were calculated as $\Delta F/F_0$ ($\Delta F = F - F_0$) for each cell. F_0 means the baseline fluorescence signal calculated by averaging lowest 30 % of all fluorescence signals from individual traces. Responding neurons were defined as neurons with fluorescence change > 30 % of F_0, and I further analyzed only responding neurons. To determine the tuning properties of each cell for each stimulus, I defined and computed preference index (PI) that ranges from 0 to 1. Preference index of cell *i* for stimulus *j* (PI_{ij}) was defined as

$$\boldsymbol{PI_{ij}} = \frac{\overline{\boldsymbol{P_{ij\cdot}}}}{\boldsymbol{Max_i}}$$

, where $\overline{P_{ij\cdot}}$ is the mean of the peak values of cell *i* for stimulus *j* across repeated trials (P_{ijk}) and P_{ijk} was determined as the highest value of amplitude during each trial *k* for stimulus *j* in cell *i*. $\boldsymbol{Max_i}$ is the highest value that cell *i* showed during the experiments. I defined cell *i* to be "preferentially responsive" or "tuned" to stimulus *j* when PI_{ij} is larger than $0.8 * \overline{PI_{i\cdot}}$, where $\overline{PI_{i\cdot}}$ is the average of PI_{ij} for all the given stimulus. Response index (RI) was defined the same as

PI except that RI is computed for one kind of stimulus (noxious) with different intensities rather than different kind of stimuli. To represent population activity patterns of S1 neurons to different stimuli in the low dimensional space, principal component analysis (PCA), a dimensionality reduction method, was used. N-dimensional activity patterns (n, number of cells) over time were projected onto their two or three principal component axes (each axis being a linear combination of n neural activities). In order to understand the encoding strategy of S1 neurons for each stimulus, I constructed scatter-plots of PI values (PI scatter plots) between each pair of two stimuli. Then, the Euclidean distances were computed and averaged between each scatter-plotted point and "equally tuned" line which passes through points of 'stimulus 1 = stimulus 2'. To standardize the average distance for each pair of stimuli, 100,000 reshuffled pairs of PIs were constructed for each pair of stimuli. The reshuffled pairs of PIs conserve the original PI values for each cell, but no associations between two PIs remain. Means and standard deviations of distances were computed from these permutation data and z-distances were calculated using the means and standard deviations. To test the significance of z-distances (i.e. whether there is any association between each pair of PIs in cells), empirical p-values were directly computed from the permutation sets and Bonferroni

corrections were conducted. To investigate whether the sensory information of the stimulus with each feature is encoded in S1 as a pattern of the population activity, I applied the supervised machine learning algorithm, k−nearest neighbor classifier (k=5, and Euclidian metric). Vectors P_{ijk} containing (i=1, …, n; n = 101 cells from 6 mice) were used as training and test samples for stimulus j. Ten−fold cross−validation was used to evaluate the decoding performance. This validation procedure ensures trained classifiers to be tested using data unseen during training phases. Empirical p−values were computed with 100,000 random permutations of the label (features to predict).

Statistics

Data were processed, analyzed and plotted using custom−written MATLAB scripts (MathWorks) or Prism software (Gragh Pad Software, USA). All data are represented as mean ± s.e.m. Two−tailed unpaired t−test (**Figure 3C, 3G**), Wilcoxon signed rank test (**Figure 4C**), two−tailed paired t−test (**Figure 4D, Figure 10C**), one−way ANOVA with Tukey's post−hoc test (**Figures 2F and 5C−E, Figure 12D**), and permutation tests with Bonferroni−corrections (**Figure 6B and 6C**) were used to determine the significance in statistical comparisons. The differences were considered significant

if a p value is below 0.05. NS indicates $p > 0.05$, * indicates $p < 0.05$, ** indicates $p < 0.01$, *** and $^{###}$ indicates $p < 0.001$.

REFERENCES

Alles, S.R.A., Bandet, M.V., Eppler, K., Noh, M.C., Winship, I.R., Baker, G., et al. (2017). Acute anti-allodynic action of gabapentin in dorsal horn and primary somatosensory cortex: Correlation of behavioural and physiological data. *Neuropharmacology* 113(Pt A), 576-590. doi: 10.1016/j.neuropharm.2016.11.011.

Apkarian, A.V., Bushnell, M.C., Treede, R.D., and Zubieta, J.K. (2005). Human brain mechanisms of pain perception and regulation in health and disease. *Eur J Pain* 9(4), 463-484. doi: 10.1016/j.ejpain.2004.11.001.

Apkarian, A.V., and Shi, T. (1994). Squirrel monkey lateral thalamus. I. Somatic nociresponsive neurons and their relation to spinothalamic terminals. *J Neurosci* 14(11 Pt 2), 6779-6795.

Basbaum, A.I., Bautista, D.M., Scherrer, G., and Julius, D. (2009). Cellular and molecular mechanisms of pain. *Cell* 139(2), 267-284. doi: 10.1016/j.cell.2009.09.028.

Bornhovd, K., Quante, M., Glauche, V., Bromm, B., Weiller, C., and Buchel, C. (2002). Painful stimuli evoke different stimulus-response functions in the amygdala, prefrontal, insula and somatosensory cortex: a single-trial fMRI study. *Brain* 125(Pt 6), 1326-1336.

Bourgeon, S., Depeault, A., Meftah el, M., and Chapman, C.E. (2016). Tactile texture signals in primate primary somatosensory cortex and their relation to subjective roughness intensity. *J Neurophysiol* 115(4), 1767-1785. doi: 10.1152/jn.00303.2015.

Bushnell, M.C., Duncan, G.H., Hofbauer, R.K., Ha, B., Chen, J.I., and Carrier, B. (1999). Pain perception: is there a role for primary somatosensory cortex? *Proc Natl Acad Sci U S A* 96(14), 7705-7709.

Carter, A.W., Chen, S.C., Lovell, N.H., Vickery, R.M., and Morley, J.W. (2014). Convergence across tactile afferent types in primary and secondary somatosensory cortices. *PLoS One* 9(9), e107617. doi: 10.1371/journal.pone.0107617.

Chu, M.W., Li, W.L., and Komiyama, T. (2016). Balancing the Robustness and Efficiency of Odor Representations during Learning. *Neuron* 92(1), 174-186. doi: 10.1016/j.neuron.2016.09.004.

Chung, J.M., Surmeier, D.J., Lee, K.H., Sorkin, L.S., Honda, C.N., Tsong, Y., et al. (1986). Classification of primate spinothalamic and somatosensory thalamic neurons based on cluster analysis. *J Neurophysiol* 56(2), 308-327. doi: 10.1152/jn.1986.56.2.308.

Cichon, J., Blanck, T.J.J., Gan, W.B., and Yang, G. (2017). Activation of cortical somatostatin interneurons prevents the development of neuropathic pain. *Nat Neurosci* 20(8), 1122-1132. doi: 10.1038/nn.4595.

Costigan, M., Scholz, J., and Woolf, C.J. (2009). Neuropathic pain: a maladaptive response of the nervous system to damage. *Annu Rev Neurosci* 32, 1-32. doi: 10.1146/annurev.neuro.051508.135531.

Craig, A.D. (2003). Pain mechanisms: labeled lines versus convergence in central processing. *Annu Rev Neurosci* 26, 1-30. doi:

10.1146/annurev.neuro.26.041002.131022.
Eroglu, C., Allen, N.J., Susman, M.W., O'Rourke, N.A., Park, C.Y., Ozkan, E., et al. (2009). Gabapentin receptor alpha2delta-1 is a neuronal thrombospondin receptor responsible for excitatory CNS synaptogenesis. *Cell* 139(2), 380-392. doi: 10.1016/j.cell.2009.09.025.
Eto, K., Wake, H., Watanabe, M., Ishibashi, H., Noda, M., Yanagawa, Y., et al. (2011). Inter-regional contribution of enhanced activity of the primary somatosensory cortex to the anterior cingulate cortex accelerates chronic pain behavior. *J Neurosci* 31(21), 7631-7636. doi: 10.1523/JNEUROSCI.0946-11.2011.
Ferrington, D.G., Downie, J.W., and Willis, W.D., Jr. (1988). Primate nucleus gracilis neurons: responses to innocuous and noxious stimuli. *J Neurophysiol* 59(3), 886-907. doi: 10.1152/jn.1988.59.3.886.
Gaese, B.H., and Ostwald, J. (2001). Anesthesia changes frequency tuning of neurons in the rat primary auditory cortex. *J Neurophysiol* 86(2), 1062-1066. doi: 10.1152/jn.2001.86.2.1062.
Garion, L., Dubin, U., Rubin, Y., Khateb, M., Schiller, Y., Azouz, R., et al. (2014). Texture coarseness responsive neurons and their mapping in layer 2-3 of the rat barrel cortex in vivo. *Elife* 3, e03405. doi: 10.7554/eLife.03405.
Goltstein, P.M., Montijn, J.S., and Pennartz, C.M. (2015). Effects of isoflurane anesthesia on ensemble patterns of Ca2+ activity in mouse v1: reduced direction selectivity independent of increased correlations in cellular activity. *PLoS One* 10(2), e0118277. doi: 10.1371/journal.pone.0118277.
Gustin, S.M., Peck, C.C., Cheney, L.B., Macey, P.M., Murray, G.M., and Henderson, L.A. (2012). Pain and plasticity: is chronic pain always associated with somatosensory cortex activity and reorganization? *J Neurosci* 32(43), 14874-14884. doi: 10.1523/JNEUROSCI.1733-12.2012.
Gwak, Y.S., and Hulsebosch, C.E. (2011). Neuronal hyperexcitability: a substrate for central neuropathic pain after spinal cord injury. *Curr Pain Headache Rep* 15(3), 215-222. doi: 10.1007/s11916-011-0186-2.
Gwak, Y.S., Kim, H.K., Kim, H.Y., and Leem, J.W. (2010). Bilateral hyperexcitability of thalamic VPL neurons following unilateral spinal injury in rats. *J Physiol Sci* 60(1), 59-66. doi: 10.1007/s12576-009-0066-2.
Hao, J.X., Kupers, R.C., and Xu, X.J. (2004). Response characteristics of spinal cord dorsal horn neurons in chronic allodynic rats after spinal cord injury. *J Neurophysiol* 92(3), 1391-1399. doi: 10.1152/jn.00121.2004.
Jin, Y., Dougherty, S.E., Wood, K., Sun, L., Cudmore, R.H., Abdalla, A., et al. (2016). Regrowth of Serotonin Axons in the Adult Mouse Brain Following Injury. *Neuron* 91(4), 748-762. doi: 10.1016/j.neuron.2016.07.024.
Johansson, R.S., Landstrom, U., and Lundstrom, R. (1982). Responses of mechanoreceptive afferent units in the glabrous skin of the human hand to sinusoidal skin displacements. *Brain Res* 244(1), 17-25.

Johnson, D.A., and Lajtha, A. (2007). *Handbook of neurochemistry and molecular neurobiology. Sensory neurochemistry.* New York: Springer.

Kenshalo, D.R., Iwata, K., Sholas, M., and Thomas, D.A. (2000). Response properties and organization of nociceptive neurons in area 1 of monkey primary somatosensory cortex. *J Neurophysiol* 84(2), 719-729. doi: 10.1152/jn.2000.84.2.719.

Kim, C.E., Kim, Y.K., Chung, G., Jeong, J.M., Lee, D.S., Kim, J., et al. (2014). Large-scale plastic changes of the brain network in an animal model of neuropathic pain. *Neuroimage* 98, 203-215. doi: 10.1016/j.neuroimage.2014.04.063.

Kim, H.Y., Kim, K., Li, H.Y., Chung, G., Park, C.K., Kim, J.S., et al. (2010). Selectively targeting pain in the trigeminal system. *Pain* 150(1), 29-40. doi: 10.1016/j.pain.2010.02.016.

Kim, S.K., and Nabekura, J. (2011). Rapid synaptic remodeling in the adult somatosensory cortex following peripheral nerve injury and its association with neuropathic pain. *J Neurosci* 31(14), 5477-5482. doi: 10.1523/JNEUROSCI.0328-11.2011.

Kim, Y.R., Kim, C.E., Yoon, H., Kim, S.K., and Kim, S.J. (2019). S1 Employs Feature-Dependent Differential Selectivity of Single Cells and Distributed Patterns of Populations to Encode Mechanosensations. *Front Cell Neurosci* 13, 132. doi: 10.3389/fncel.2019.00132.

Kim, Y.S., Anderson, M., Park, K., Zheng, Q., Agarwal, A., Gong, C., et al. (2016). Coupled Activation of Primary Sensory Neurons Contributes to Chronic Pain. *Neuron* 91(5), 1085-1096. doi: 10.1016/j.neuron.2016.07.044.

Kopach, O., Viatchenko-Karpinski, V., Belan, P., and Voitenko, N. (2012). Development of inflammation-induced hyperalgesia and allodynia is associated with the upregulation of extrasynaptic AMPA receptors in tonically firing lamina II dorsal horn neurons. *Front Physiol* 3, 391. doi: 10.3389/fphys.2012.00391.

Lamour, Y., Willer, J.C., and Guilbaud, G. (1983). Rat somatosensory (SmI) cortex: I. Characteristics of neuronal responses to noxious stimulation and comparison with responses to non-noxious stimulation. *Exp Brain Res* 49(1), 35-45.

Lefort, S., Tomm, C., Floyd Sarria, J.C., and Petersen, C.C. (2009). The excitatory neuronal network of the C2 barrel column in mouse primary somatosensory cortex. *Neuron* 61(2), 301-316. doi: 10.1016/j.neuron.2008.12.020.

Light, A.R., Trevino, D.L., and Perl, E.R. (1979). Morphological features of functionally defined neurons in the marginal zone and substantia gelatinosa of the spinal dorsal horn. *J Comp Neurol* 186(2), 151-171. doi: 10.1002/cne.901860204.

Lorenz, J., Cross, D.J., Minoshima, S., Morrow, T.J., Paulson, P.E., and Casey, K.L. (2002). A unique representation of heat allodynia in the human brain. *Neuron* 35(2), 383-393.

Matsumoto, N., Sato, T., Yahata, F., and Suzuki, T.A. (1987). Physiological properties of tooth pulp-driven neurons in the first somatosensory cortex (SI) of the cat. *Pain* 31(2), 249-262.

Milenkovic, N., Zhao, W.J., Walcher, J., Albert, T., Siemens, J., Lewin, G.R., et al. (2014). A somatosensory circuit for cooling perception in mice. *Nat Neurosci* 17(11), 1560-1566. doi: 10.1038/nn.3828.

Moayedi, M., and Davis, K.D. (2013). Theories of pain: from specificity to gate control. *J Neurophysiol* 109(1), 5-12. doi: 10.1152/jn.00457.2012.

Moehring, F., Cowie, A.M., Menzel, A.D., Weyer, A.D., Grzybowski, M., Arzua, T., et al. (2018). Keratinocytes mediate innocuous and noxious touch via ATP-P2X4 signaling. *Elife* 7. doi: 10.7554/eLife.31684.

Otazu, G.H., Chae, H., Davis, M.B., and Albeanu, D.F. (2015). Cortical Feedback Decorrelates Olfactory Bulb Output in Awake Mice. *Neuron* 86(6), 1461-1477. doi: 10.1016/j.neuron.2015.05.023.

Parthasarathy, A., Herikstad, R., Bong, J.H., Medina, F.S., Libedinsky, C., and Yen, S.C. (2017). Mixed selectivity morphs population codes in prefrontal cortex. *Nat Neurosci* 20(12), 1770-1779. doi: 10.1038/s41593-017-0003-2.

Paul, R.L., Merzenich, M., and Goodman, H. (1972). Representation of slowly and rapidly adapting cutaneous mechanoreceptors of the hand in Brodmann's areas 3 and 1 of Macaca mulatta. *Brain Res* 36(2), 229-249.

Perl, E.R. (2007). Ideas about pain, a historical view. *Nat Rev Neurosci* 8(1), 71-80. doi: 10.1038/nrn2042.

Poisbeau, P., Patte-Mensah, C., Keller, A.F., Barrot, M., Breton, J.D., Luis-Delgado, O.E., et al. (2005). Inflammatory pain upregulates spinal inhibition via endogenous neurosteroid production. *J Neurosci* 25(50), 11768-11776. doi: 10.1523/JNEUROSCI.3841-05.2005.

Prescott, S.A., Ma, Q., and De Koninck, Y. (2014). Normal and abnormal coding of somatosensory stimuli causing pain. *Nat Neurosci* 17(2), 183-191. doi: 10.1038/nn.3629.

Price, D.D., Greenspan, J.D., and Dubner, R. (2003). Neurons involved in the exteroceptive function of pain. *Pain* 106(3), 215-219.

Quiton, R.L., Masri, R., Thompson, S.M., and Keller, A. (2010). Abnormal activity of primary somatosensory cortex in central pain syndrome. *J Neurophysiol* 104(3), 1717-1725. doi: 10.1152/jn.00161.2010.

Ramirez-Cardenas, A., and Viswanathan, P. (2016). The Role of Prefrontal Mixed Selectivity in Cognitive Control. *J Neurosci* 36(35), 9013-9015. doi: 10.1523/JNEUROSCI.1816-16.2016.

Reed, J.L., Pouget, P., Qi, H.X., Zhou, Z., Bernard, M.R., Burish, M.J., et al. (2008). Widespread spatial integration in primary somatosensory cortex. *Proc Natl Acad Sci U S A* 105(29), 10233-10237. doi: 10.1073/pnas.0803800105.

Rigotti, M., Barak, O., Warden, M.R., Wang, X.J., Daw, N.D., Miller, E.K., et al. (2013). The importance of mixed selectivity in complex cognitive tasks. *Nature* 497(7451), 585-590. doi: 10.1038/nature12160.

Saal, H.P., and Bensmaia, S.J. (2014). Touch is a team effort: interplay of submodalities in cutaneous sensibility. *Trends Neurosci* 37(12), 689-697. doi: 10.1016/j.tins.2014.08.012.

Seifert, F., and Maihofner, C. (2009). Central mechanisms of experimental and chronic neuropathic pain: findings from functional imaging studies.

Cell Mol Life Sci 66(3), 375-390. doi: 10.1007/s00018-008-8428-0.
Sekiguchi, K.J., Shekhtmeyster, P., Merten, K., Arena, A., Cook, D., Hoffman, E., et al. (2016). Imaging large-scale cellular activity in spinal cord of freely behaving mice. *Nat Commun* 7, 11450. doi: 10.1038/ncomms11450.
Senapati, A.K., Huntington, P.J., LaGraize, S.C., Wilson, H.D., Fuchs, P.N., and Peng, Y.B. (2005). Electrical stimulation of the primary somatosensory cortex inhibits spinal dorsal horn neuron activity. *Brain Res* 1057(1-2), 134-140. doi: 10.1016/j.brainres.2005.07.044.
Sur, M., Wall, J.T., and Kaas, J.H. (1984). Modular distribution of neurons with slowly adapting and rapidly adapting responses in area 3b of somatosensory cortex in monkeys. *J Neurophysiol* 51(4), 724-744. doi: 10.1152/jn.1984.51.4.724.
Timmermann, L., Ploner, M., Haucke, K., Schmitz, F., Baltissen, R., and Schnitzler, A. (2001). Differential coding of pain intensity in the human primary and secondary somatosensory cortex. *J Neurophysiol* 86(3), 1499-1503. doi: 10.1152/jn.2001.86.3.1499.
Vierck, C.J., Whitsel, B.L., Favorov, O.V., Brown, A.W., and Tommerdahl, M. (2013). Role of primary somatosensory cortex in the coding of pain. *Pain* 154(3), 334-344. doi: 10.1016/j.pain.2012.10.021.
Whitsel, B.L., Favorov, O.V., Li, Y., Lee, J., Quibrera, P.M., and Tommerdahl, M. (2010). Nociceptive afferent activity alters the SI RA neuron response to mechanical skin stimulation. *Cereb Cortex* 20(12), 2900-2915. doi: 10.1093/cercor/bhq039.
Woolf, C.J., American College of, P., and American Physiological, S. (2004). Pain: moving from symptom control toward mechanism-specific pharmacologic management. *Ann Intern Med* 140(6), 441-451.
Zimmerman, A., Bai, L., and Ginty, D.D. (2014). The gentle touch receptors of mammalian skin. *Science* 346(6212), 950-954. doi: 10.1126/science.1254229.

Abstract in Korean (국문 초록)

생리 및 병리적 조건에서 촉각과 통증에 대한 일차 체성감각 피질의 암호화 전략

김 유 림
서울대학교 대학원
의과대학 의과학과 (생리학 전공)

일차 체성감각 피질은 촉각과 통증을 지각하고 구별하는 데에 있어서 매우 중요한 역할을 한다. 전통적으로, 일차 체성감각피질을 포함한 체성감각계의 신경세포는 브러쉬, 핀치와 같은 무해한 자극과 유해한 자극에 대한 그 세포의 전기생리학적 반응에 따라 저역치, 고역치 또는 광동적범위 신경세포로 분류되어 왔다. 브러쉬와 포셉을 이용한 이 자극은 '유해성' 뿐만 아니라 브러쉬와 포셉의 '촉감', 동적/정적인 '역동성'과 같은 다른 특성들도 포함하고 있다. 하지만 감각 자극의 이렇게 다양한 특성들을 일차 체성감각피질의 개별세포와 집단 수준에서 종합적으로 어떻게 부호화하고 있는 지에 대한 연구는 부족하다.

조직 및 신경 손상은 이질통, 통각 과민과 같은 과민증을 동반하는 염증성 또는 신경병성 통증을 초래한다. 하지만 통증 과민성일 때 무해하고 유해한 기계적 자극에 대한 일차 체성감각 피질 신경 세포의 반응 속성이 어떻게 달라지며, 이 변화가 통각 과민증과 어떻게 연관되어 있는 지에 대한 연구는 부족하다.

나는 일차 체성감각 피질 세포가 촉각과 통증에 대한 다양한 자극 특성을 동시다발적으로 어떻게 암호화 하고 있는 지 조사했다. 또한 촉각 및 통증 자극에 대한 그 세포들의 반응 속성이 통증 과민증 일 때 어떻게 달라지는 지 조사했다. 이 조사를 위해, 나는 이광자 칼슘 이미징을 통해 무해하고, 유해한 촉각 및 통증 자극을 생쥐의 발바닥에 가하면서

생쥐의 일차 체성감각 피질 신경세포의 칼슘 반응을 기록했다.

이 논문은 촉각 및 통증 자극에 대한 일차 체성감각 피질 세포의 반응 속성을 설명하는 두 가지 부분으로 구성되어 있다. 제 1장에서는, 일차 체성감각 피질 신경세포가 촉감이 다른 자극에 대해서 높은 선택적 반응을 보인 것을 확인했다. 하지만 역동성 또는 유해성 특성에 대해서는 낮은 선택성을 보였으며, 그 중 역동성에 약간 더 높은 선택성을 보인 것을 확인했다. 제 2장에서는, 통증 과민증 일 때, 유해-선호 신경세포가 무해한 촉각 자극에도 반응하는 것을 확인했다. 하지만, 촉각 및 통증 자극 모두에 반응한 세포 (광범위하게 조정된 세포)는 자극에 대한 튜닝 속성이 과민증일 때 유지됐고, 그 세포의 일부는 촉각 및 통증 자극에 대한 반응성이 증가했다.

이 논문은 일차 체성감각 피질 신경세포가 자극 특성-의존적 방식으로 특이성 부호화와 패턴 부호화의 혼합 된 전략을 사용하는 걸 제시했다. 또한, 통증 과민증 일 때, 일체 체성감각 피질은 자극에 대한 반응 속성이 바뀌고, 광범위하게 조정된 세포의 반응성이 전반적으로 증가하는 방식으로 과민증에 기여하고 있다는 것을 보여줬다. 본 논문은 생리 및 병리적 조건에서 촉각 및 통증 자극에 대한 일차 체성감각 피질의 암호화 전략과 반응 속성에 대해 이해하기 위한 중요한 정보를 제공한다.

핵심어: 촉각, 통증, 일차 체성감각피질, 신경 부호화, 이광자 칼슘 이미징, 자극 특성, 과민증
학번: 2010-23737